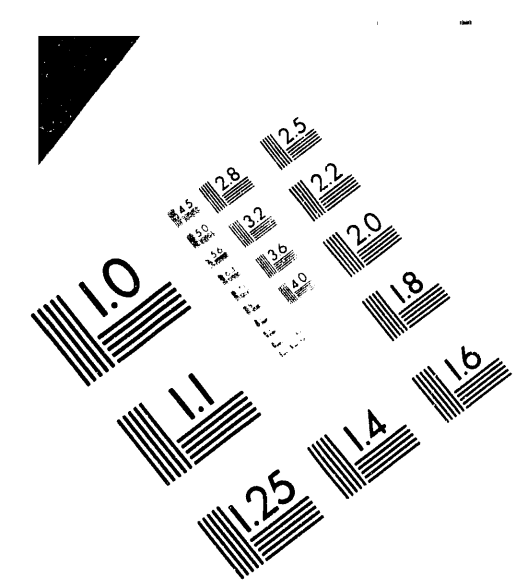

Association for Information and Image Management

1100 Wayne Avenue, Suite 1100
Silver Spring, Maryland 20910

301/587-8202

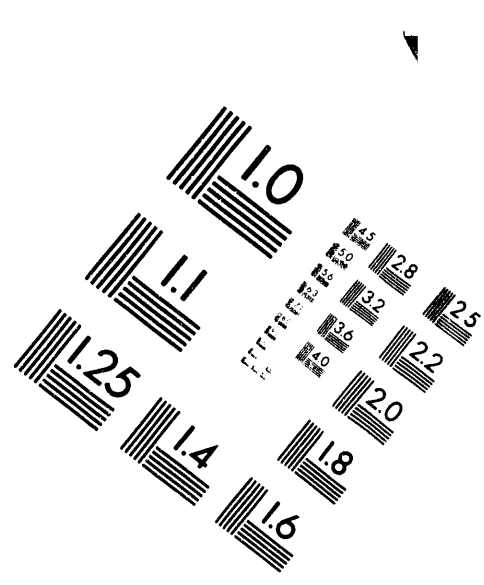

Centimeter

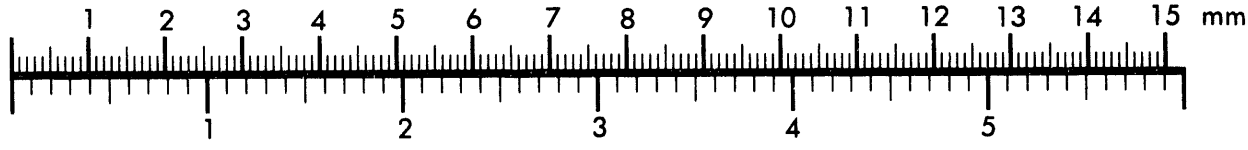

Inches

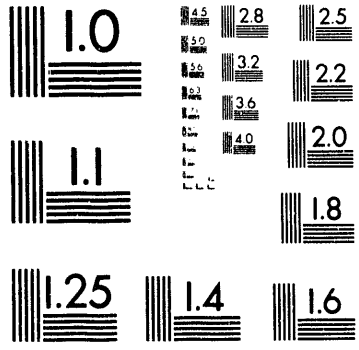

MANUFACTURED TO AIIM STANDARDS
BY APPLIED IMAGE, INC.

1 of 1

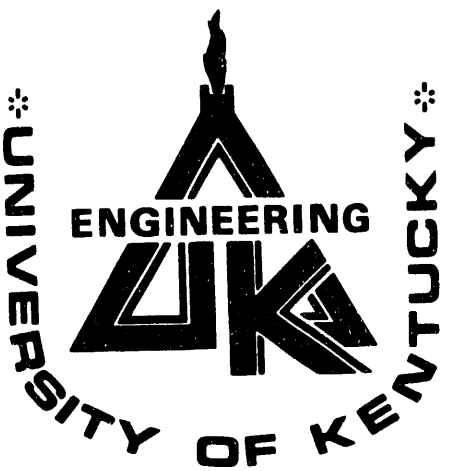

DETERMINATION OF LOCAL RADIATIVE PROPERTIES IN COAL-FIRED FLAMES

(Grant No: DE-FG22-87PC79916)

TECHNICAL PROGRESS REPORT - DOE/PC/79916-3

THE FIRST YEAR : 9/15/1987 - 9/15/1988

Submitted to the

U.S. Department of Energy
Pittsburgh Energy Technology Center

M. Pinar Mengüç

Department of Mechanical Engineering
College of Engineering
University of Kentucky
Lexington, Kentucky 40506-0046

DETERMINATION OF LOCAL RADIATIVE PROPERTIES IN COAL-FIRED FLAMES

(Grant No: DE-FG22-87PC79916)

TECHNICAL PROGRESS REPORT - DOE/PC/79916-3

THE FIRST YEAR : 9/15/1987 - 9/15/1988

Submitted to the

U.S. Department of Energy
Pittsburgh Energy Technology Center

M. Pinar Mengüç

DISCLAIMER

DETERMINATION OF LOCAL RADIATIVE PROPERTIES IN COAL-FIRED FLAMES

(Grant No: DE-FG22-87PC79916)

TECHNICAL PROGRESS REPORT - DOE/PC/79916-3

FIRST YEAR : SEPTEMBER 15, 1987 - SEPTEMBER 15, 1988

Submitted to the

U.S. Department of Energy
Pittsburgh Energy Technology Center

by

M. Pinar Mengüç (Principal Investigator)

B. Agarwal (Graduate Student)
M. Bush (Graduate Student)
D. Dsa (Graduate Student)
S. Subramaniam (Graduate Student)

Department of Mechanical Engineering
University of Kentucky
Lexington, KY 40506-0046

TABLE OF CONTENTS

PREFACE

This report presents results of research on determining the radiative properties of coal particles under a grant from the U.S. Department of Energy Pittsburgh Energy Technology Center (Grant No: DE-FG22-87PC79916). The report covers the period September 15, 1987 through September 15, 1988, which is the first year of the three year program. Because the grant started in the middle of the fall semester, we did not have any graduate students working on the project until January 1, 1988. Originally, Professor R.A. Altenkirch was also involved with the project as a co-principal investigator. However, in June 1988 he resigned from the University of Kentucky to become the Dean of College of Engineering at Mississippi State University. Instead of directing funds to another faculty member, we chose to hire more graduate students to work on this project. In addition to four students involved on the project, one other student will start working on this research in January 1989. It is also important to note that, we obtained partial support from University of Kentucky Center for Computational Sciences (for S. Subramaniam), from Department of Mechanical Engineering (for B. Agarwal, D. Dsa, and S. Subramaniam) and from NSF Grant CBT-8708679 (for B. Agarwal) during the first year to support graduate students.

The report is divided to two parts. In the first one, we discuss the analytical studies performed so far. We do not give the details of the tomographic reconstruction technique here because it was discussed in our first report. On the other hand, detailed description of other analytical works will be given in upcoming journal papers. In the second part of the report, the development of an experimental test cell and preliminary experiments are discussed in addition to the literature survey of related works.

1. INTRODUCTION

Radiation transfer is the most significant mode of heat transfer in large scale pulverized-coal fired furnaces. In order to improve the efficiency of these systems, radiation heat transfer should be modeled accurately. In predicting the radiative heat flux distribution in practical systems, three important problems must be considered simultaneously: i) mathematical formulation and solution of the radiative transfer equation (RTE), ii) modeling of spectrally banded radiation from the combustion gases, and iii) modeling of continuum radiation from the particles such as soot, pulverized-coal, char, and fly-ash in the combustion products. In addition to these, the interaction of radiation with combustion and with turbulence should be accounted for (Faeth et al., 1985). Recently, an extensive, in-depth review of the modeling of radiation heat transfer in combustion chambers has been prepared (Viskanta and Menguc, 1987); therefore, there is no need to repeat that material here.

It is already known that the most important missing link in the prediction of radiation heat transfer in combustion systems is the lack of detailed information about the optical and physical properties of combustion products (Viskanta and Menguc, 1987). The purpose of this research is to determine the radiative properties of coal particles. Considering the uncertainty in the fundamental optical and physical properties of coal particles, such as complex index of refraction, size, size distribution, and shape, it is difficult to predict the radiative properties of particles using available analytical methods, such as Lorenz-Mie theory. For a better understanding of radiation and radiation/combustion or radiation/turbulence interactions, it is preferable to determine the radiative properties *in situ*.

The radiative properties of particles can be calculated rigorously from Lorenz-Mie theory (van de Hulst, 1981; Bohren and Huffman, 1983) for particles that are either spherical or long and cylindrical in shape. For other shapes, the properties can be determined using the extended boundary condition (T-matrix) method (Waterman, 1971; Barber and Yeh, 1975). The latter method is too tedious to be used in practical systems, and its use cannot be justified unless the shapes of the particles are well defined. If the particles are assumed to be spherical or cylindrical, then Lorenz-

Mie calculations can be easily performed to predict the radiative properties, provided that the spectral complex index of refraction of the particles and the local particle volume fraction (or number density) in the medium are available. The assumption of spherical shape for combustion generated particles is widely employed, and it is usually acceptable because the particle size distribution washes away most of the non-uniform shape effects to yield radiative properties close to those for spherically shaped particles (Kerker, 1969; Chylek, et al., 1976). It is the uncertainty in the complex index of refraction of the particles and their local volume fraction in a combustion chamber that are the main sources of error in predicting radiative properties.

In particle laden flames, the particle radiative properties are more critical than those of the gases because particles absorb, emit, and scatter radiation within the entire wavelength spectrum, while gases contribute only in certain spectral bands. The particle properties, however, are usually approximated, rather than accurately predicted, because of *a priori* assumptions about the spectral complex index of refraction, particle shape, size, and particle concentration distributions. There are some fundamental studies available in the literature where soot and fly-ash complex index of refraction data were obtained by applying the classical reflection/transmission measurement technique to thin, compressed soot or fly-ash wafers (Felske et al., 1985; Goodwin, 1986). Although it was shown by Felske et al. (1985) that the soot optical properties can accurately be obtained from such measurements, it is difficult to say whether or not the complex index of refraction of the micron-size fly-ash particles suspended within the hot combustion gases would be the same as the compressed wafers.

In order to study the interaction of radiation with combustion or turbulence in combustion systems, we have to know the medium radiative properties as accurately as possible. We cannot afford to use some "guessed" values for the complex index of refraction, shape, size, and concentration distributions of the particles to draw conclusions about micro-scale radiation-turbulence or radiation-combustion interactions. The reason we need to know the complex index of refraction and the size of the particles is to determine the radiative properties using the established theoretical models, such as Lorenz-Mie theory. It is also important to note that to study such fundamental

interactions, we have to know the local radiative properties, not the complex index of refraction of the particles. It is required for the calculations of absorption, extinction, and scattering cross sections, and the scattering phase function using Lorenz-Mie theory or the T-matrix method, and to perform these calculations the particle size and shape is to be approximated. It means that, even if we have accurate values for the spectral complex index of refraction and size of the particles, a significant portion of that information will be lost because of the shape and concentration distribution approximations made.

With these facts in mind, it is possible to propose an "effective radiative property" concept for the particles in practical systems. These effective properties can be obtained from a detailed experimental/analytical procedure. First, a series of experiments will be performed, and the attenuation and scattering of incident radiation at several angular orientations will be recorded. The physical and optical characteristics of the total particle cloud determines the amount of attenuation, and this information will be carried in the measured projection data. Effective properties can be determined by solving the inverse radiation problem in a corresponding geometry using these projection data as input. Following this, empirical relations for "effective radiative properties" can be derived for given physical conditions. This can be achieved if other physical properties, such as volume fraction and particle size distribution, temperature of the particles and combustion gases, and concentration distribution of gases, can be predicted from theory or parallel experiments, and their contribution to the experimental data is quantified. It is worth noting that many researchers have intuitively used the effective property concept to calculate the radiative properties in inhomogeneous media, usually by assigning mean values to different parameters such as diameter, complex index of refraction, local volume fraction composition and others (see, e.g., Menguc and Viskanta, 1986). However, in the literature, there is no fundamental study based on experiments from which the radiative properties of particle clouds that scatter the radiation can be obtained.

In complicated practical systems, the medium is usually inhomogeneous, and. therefore, analytical inversion of the radiative transfer equation in order to determine the radiative properties is

almost impossible to achieve. If the medium is assumed to be absorbing, emitting, non- or only-forward-scattering, then the solution of the inverse radiation problem in a one-dimensional geometry will yield the desired effective properties. If the medium is cylindrical and axisymmetric, then the solution of the inverse radiation problem is obtained by solving the Abel integral equation (Cremers and Birkebak, 1966; Chakravarty et al., 1988). Although the axisymmetric configuration can be realized for most particle-laden flames, the situation where the particles are non-scattering or scatter only-in-the-forward direction cannot. However, even a slight perturbation from non-scattering to, for example, predominantly-forward-scattering, makes the problem significantly more complicated, and none of the conventional models can be used to solve the resulting inverse radiation problem.

2. ANALYTICAL STUDIES

One of the main goals of this study is to develop an analytical procedure to determine the "effective radiative properties" of cylindrical axisymmetric, inhomogeneous, absorbing, and anisotropically scattering clouds using the data from line-of-sight measurements. These "projection data" will be reduced to determine the local, effective scattering and extinction cross sections, and the scattering phase function of particles. The data reduction scheme is based on the solution of the inverse radiation problem.

The inverse radiation problem is to be formulated and solved by considering the physical system. For an absorbing, emitting, and anisotropically scattering pulverized-coal flame, the system to be considered is cylindrical and axisymmetric, but nonhomogeneous. If the medium is not scattering, the solution of the inverse problem is obtained from the Abel integral equation. For a scattering medium, however, there is no inverse solution technique available in the literature. A new technique, angular tomography, can be used for such a system provided that the medium is not a multiple scattering one. In this chapter, the formulations of the inverse solution techniques for axisymmetric systems will be discussed. In addition to that, we will briefly discuss an inverse solution technique based on a Monte-Carlo statistical approach for one-dimensional planar systems. This approach is especially useful for determining the properties of a cold stream of

coal/char particles *in-situ*, from the experiments discussed in Chapter 3.

2.1 Inverse Radiation Problem - Axisymmetric System

In order to determine the radiative properties of nonscattering media, the inverse radiation problem is solved either starting from the integral form of the radiative transfer equation (RTE) or after reducing it to the Abel integral equation. Recently, we used both of these techniques to determine the absorption coefficient profiles in a smoking ethylene-air diffusion flame (Chakravarty et al., 1988). The tomographic reconstruction technique was especially powerful for this type of inverse problem.

Tomographic reconstruction, which is the backbone of computed tomography, is based on the Radon transform (Deans, 1983; Natterer, 1987). This technique will be applied to an absorbing, emitting, scattering, and nonhomogeneous medium for the first time, and it will be called "angular tomography".

As the name suggests (in Greek, "tomos" means section), tomography is based on the measurement of the change of the radiation intensity along the sections of property field. The measurements are performed at M radial r locations and at N angular θ orientations (see Fig.1), and a line-of-sight projection from each section is recorded. If the medium is an absorbing medium, then the attenuation of radiation along the path is governed by the Boguert-Lambert law, which can be written as

$$I_\lambda(r,\theta)/I_{o,\lambda} = D_\lambda \exp\left(-\int_s \left[\sum_j N_j\, Q_{a,\lambda,j}\right] ds\right) \tag{1}$$

where $I_{o,\lambda}$ and I_λ are the initial and transmitted spectral radiation intensities at wavelength λ, respectively; N_j is number density of particles; $Q_{a,\lambda,j}$ is spectral absorption cross-section of the j-th type particles, and s is the path length of radiation. In this equation, D_λ is a parameter that carries information about the solid angle for the detector, detector sensitivity, and other proportionality factors. We can rewrite Eq.(1) as

$$-\ln \frac{I_\lambda(r,\theta)}{D_\lambda I_{o,\lambda}} = P(r,\theta) = \int_S f(x,y)\, ds \tag{2}$$

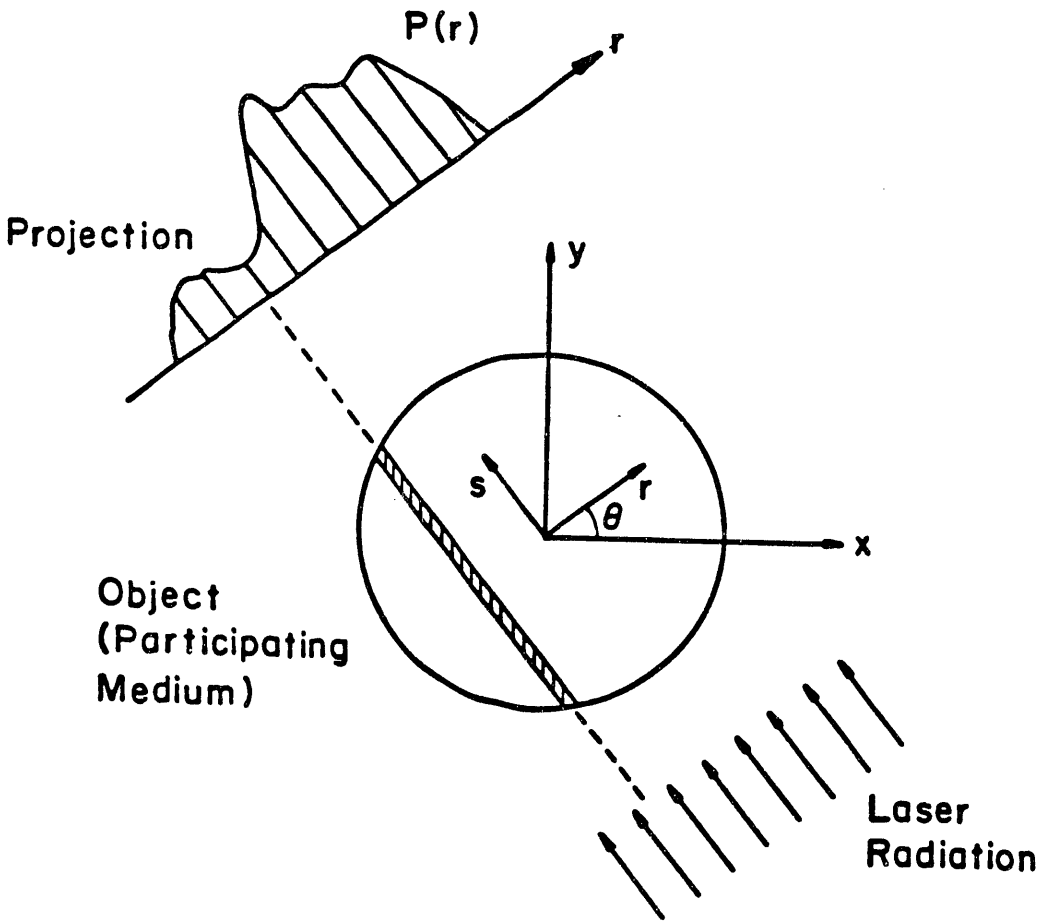

Fig.1 Coordinate System and Configuration for Projection Intensity Readings.

Here $P(r,\theta)$ is the projection for a given angle θ, and it is known because the $I_\lambda/I_{o,\lambda}$ ratio is measured experimentally. In order to estimate the accuracy of the proposed method, it is desired to evaluate it numerically. For this reason, we obtained the projection intensity, $P(r,\theta)$, for an axisymmetric, thin medium. We assumed that there is single scattering only, and the medium is comprised of several uniform-property cylindrical ring elements. Then, the radiative transfer equation along the line-of-sight is given as

$$\frac{dI}{ds} = -(\kappa+\sigma)I + \sigma p(s,0)I\frac{d\Omega}{4\pi} = -\bar{\beta}I \tag{3}$$

where

$$\bar{\beta}(s) = \beta(s)[1-\omega\frac{d\Omega}{4\pi}p(s,0)] \tag{4}$$

After a lengthy algebra (Menguc, 1988), the ratio of intensity scattered to direction ϕ by a control volume on the axis at location x_0 to the incident intensity is given as (see Fig.2)

$$I^* = \frac{I_2}{I_1} = T(x_0,\phi)S(x_0,\phi) \tag{5}$$

where T and S corresponds to transmission and scattering components, respectively, and they are given as

$$T(x_0,\phi) = T_1(x_0,\phi) + T_2(x_0,\phi) \tag{6}$$

$$T_1(x_0,\phi) = \exp[-x_0\theta_0\sum_{i=1}^{N} g_1(a_i)w_i] \tag{7a}$$

$$T_2(x_0,\phi) = \exp[-2x_0\phi\cos\phi\sum_{i=1}^{N} g_2(a_i)w_i] \tag{7b}$$

with

$$g_1(a_i) = \bar{\beta}(\frac{x_0}{\cos(\theta_0 a_i)})[1+s(\theta_0 a_i,\phi)]\frac{1}{\cos^2(\theta_0 a_i)} \tag{8a}$$

$$g_2(a_i) = \bar{\beta}(\frac{x_0\cos\phi}{\cos(\phi a_i)})\frac{1}{\cos^2(\phi a_i)} \tag{8b}$$

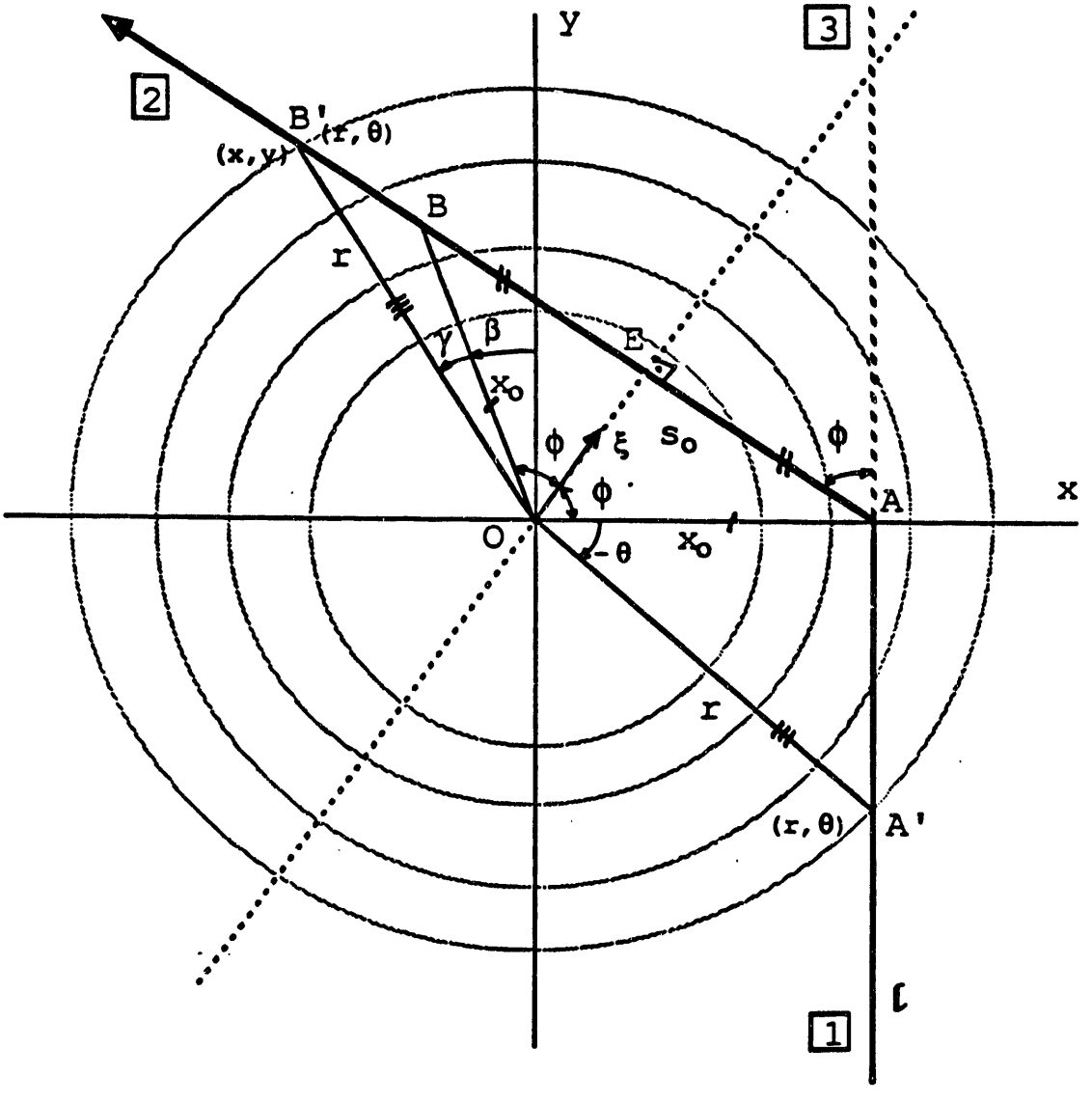

Fig.2 Coordinate system and nomenclature used for angular tomography algorithm.

and

$$S(x_0,\phi) = \sigma(x_0)\frac{p(x_0,\phi)}{4\pi}ds \tag{9}$$

where

$$s = \sin\theta[-\frac{\sin(\gamma+\beta)}{\sin\phi} + \frac{\cos(\gamma+\beta)}{\cos\phi} + (\frac{\sin(\gamma+\beta)}{\cos\phi} + \frac{\cos(\gamma+\beta)}{\sin\phi})(\frac{\sin^2\gamma-\cos^2\phi(1-\cos\gamma\cos\theta)}{\sin\gamma\cos\theta\cos^2\phi-\frac{1}{2}\sin2\gamma})] \tag{10}$$

In Figs.3 and 4, calculated theoretical distributions of transmission as a function of scattering angle are shown (for corresponding nomenclature, see Fig.2; K is a system constant). It is clear that, as the particle diameter for bituminous coal decreases, a significant change for the angular transmission is obtained. On the other hand, if the particles are large, then their contribution is mainly in the forward direction. This observation may lead us to two significant conclusions: i) if there are only coal particles in the medium, then in the experiments it is not critical to focus the laser beam to center, ii) if there are also fly-ash particles present (size of which may be less than 10 μm), then variation in angular transmission can be attributed only to the fly-ash radiative properties, which may allow us to determine their properties *in situ*.

2.2 Tomographic Reconstruction Technique

The angular transmission/scattering data displayed in Figs. 3 and 4 can be used in inverse solution schemes to determine medium effective properties. The projections at different angles can be measured by changing the orientation of the light source, i.e., by changing θ. Once the transmissivity measurements at M spatial and N angular grid points are recorded, the property field can be obtained from Eq.(2) using one of the four image construction methods, namely i) the back projection method; ii) algebraic reconstruction techniques (ART); iii) the Fourier transform method; iv) the convolution (or, filtered back projection) method (Iizuka, 1985). Although the accuracy and efficiency of these methods may change from one application to the other, the convolution method, which was originally proposed by Ramachandran and Lakshminarayanan (1971), is the most fre-

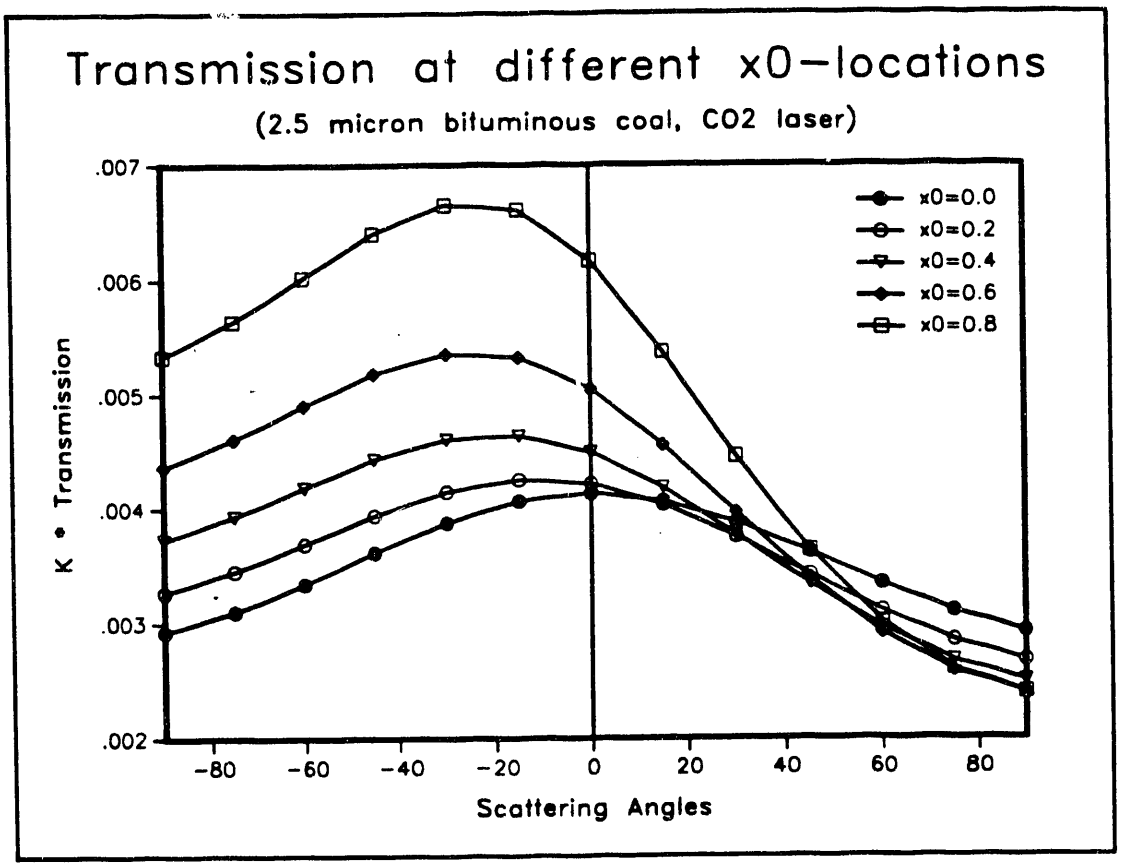

Fig.3 Variation of transmission as function of x_0 and scattering angle; from direct formulation; for optical thickness of 0.5.

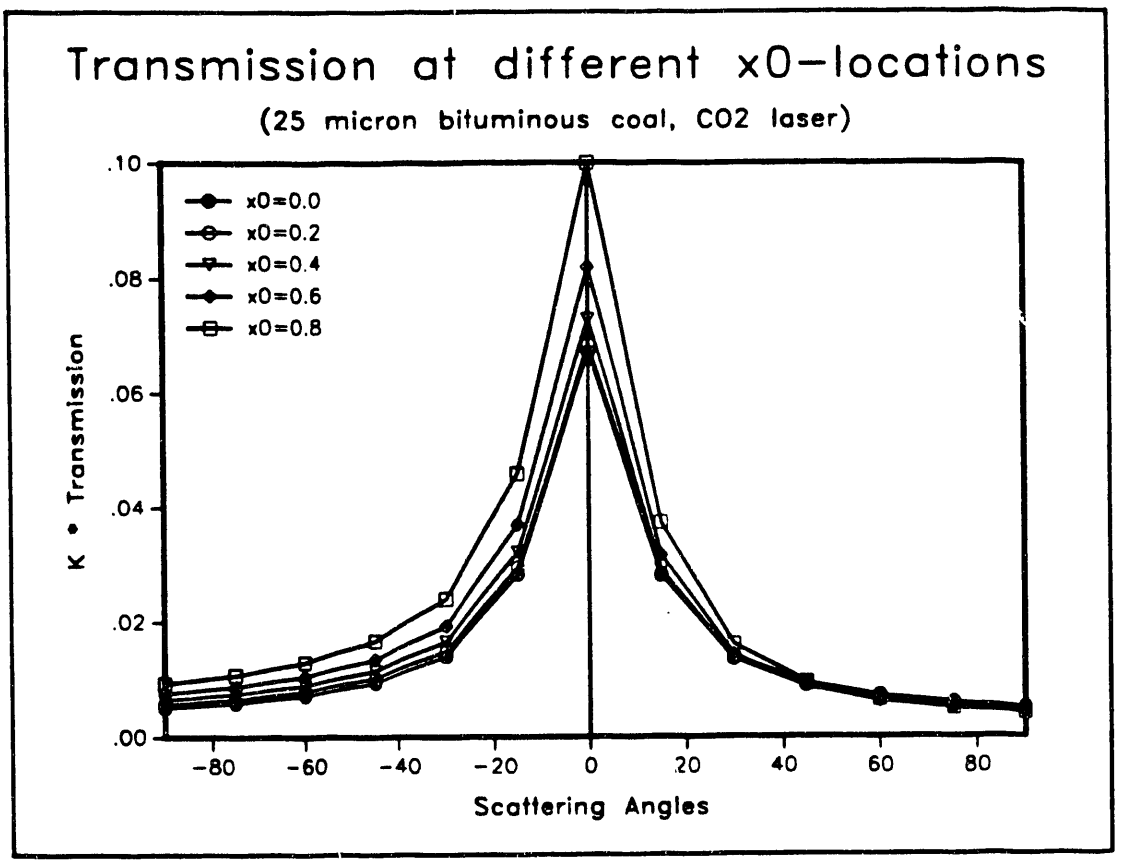

Fig. 4 Variation of transmission as function of x_0 and scattering angle; from direct formulation; for optical thickness of 0.5.

quently used method in the application of computed tomography, mainly because of its computational simplicity. Its use has been recommended unless evidence is available to the contrary in a particular application (Herman, 1980). For axisymmetric, absorbing media, it was shown that this method consistently yields accurate and stable results for reconstructed profiles (Chakravarty et al., 1988).

The projection - intensity expression, Eq.(3), can be modified to get:

$$P(l,\phi) = -ln\frac{I_2}{I_1} = \int_1^2 \bar{\beta} dz \tag{11}$$

In a classical sense, P-functions can be considered as Radon transforms of $\bar{\beta}$ functions (Deans, 1983). It is important to recognize that the path 1-2 is not a straight line, as in the definition of the Radon transform, but it is a path that is made up of segments that are piece-wise straight (see Fig. 2). Eq. (11) can also be written as:

$$P(l,\phi) = \check{f}(l,\phi) = Rf(r) = \int\int f(r)\, \delta(l-\xi\cdot z) dz \tag{12}$$

where the Dirac function is used to pick the projection intensity along the path length l, with the direction cosine ξ. In this problem, the distribution function f(r) is related to the modified extinction coefficient distribution, $\bar{\beta}$, of the medium.

2.2.1 Convolution Technique for Computed Tomography

In this section, we will follow the Fourier convolution technique of Ramachandran and Lakshminarayanan (1971) to reconstruct the $\bar{\beta}$-function given in Eq. (11) (or, say, f-function for general application) using the projection intensity readings.

The Fourier transform of Eq. (11) is

$$F(R, \Phi) = \int_{-\pi}^{\pi} P(l, \phi)\ \exp(2\pi i R l) dl \tag{13}$$

where $x_0 \equiv l$. Here the Φ-angle is equivalent to the ϕ-angle, and it corresponds to the ϕ-angle given in the paper by Ramachandran and Lakshminarayanan (1971). We choose to use bold characters for the transformed angle to differentiate the real and Fourier domains from each other.

The f-functions can be written using the inverse Fourier transform:

$$f(r, \Psi) \equiv \int_0^{2\pi} \int_0^{+\pi} F(R, \Phi) \exp\left[-2\pi i R r \cos(\Psi - \Phi)\right] R dR d\Phi \tag{14}$$

For an axisymmetric system, Ψ dependency is not required. In Eq. (11), $f(x_0, \theta)$ is to be interpreted as f(r) because each (x_0, θ) pair yields a single r-value.

The configuration for the l- and the Φ-parameters is shown on Fig. 5. The path indexed with "l" corresponds to following sum:

$$l \equiv \text{nonscattered light up to center line} + \text{scattered light in } \phi \text{ direction}$$

Here ϕ is the angle at which the detector line-of-sight is oriented with incident radiation line-of-sight, which coincides with Φ-angles.

Using this configuration, we can write "angular tomography" expressions from the regular "computed tomography" expressions. There are basically two fundamental differences between the angular tomography (AT) and computed tomography (CT):

i) In CT, the orientation of the incident beam is changing in the projection intensity plane. In AT, the incident beam orientation is fixed, although the projection intensity plane is a function of Φ (or ϕ, or θ).

ii) In the AT formulation, we have an extra term: the second term on the right-hand-side of Eq. (11).

It is important to note that in Eq. (13), we integrate the projection intensity over $l \in (-\infty, \infty)$ for a given Φ-orientation of detectors. P-projection intensities are defined by Eq. (11) for a given x_0 value. Now, following RL, we can write Eq. (14) as

$$f(r, \Psi) = \int_0^{2\pi} \int_0^{\infty} |R| F(R, \Phi) \exp[-2\pi i R r \cos(\Psi - \Phi)] dR d\Phi \tag{15}$$

If we define a new h-function

$$h(l; \Phi) = \int_{-\infty}^{\infty} |R| F(R, \Phi) \exp(-2\pi i R l) dR \tag{16}$$

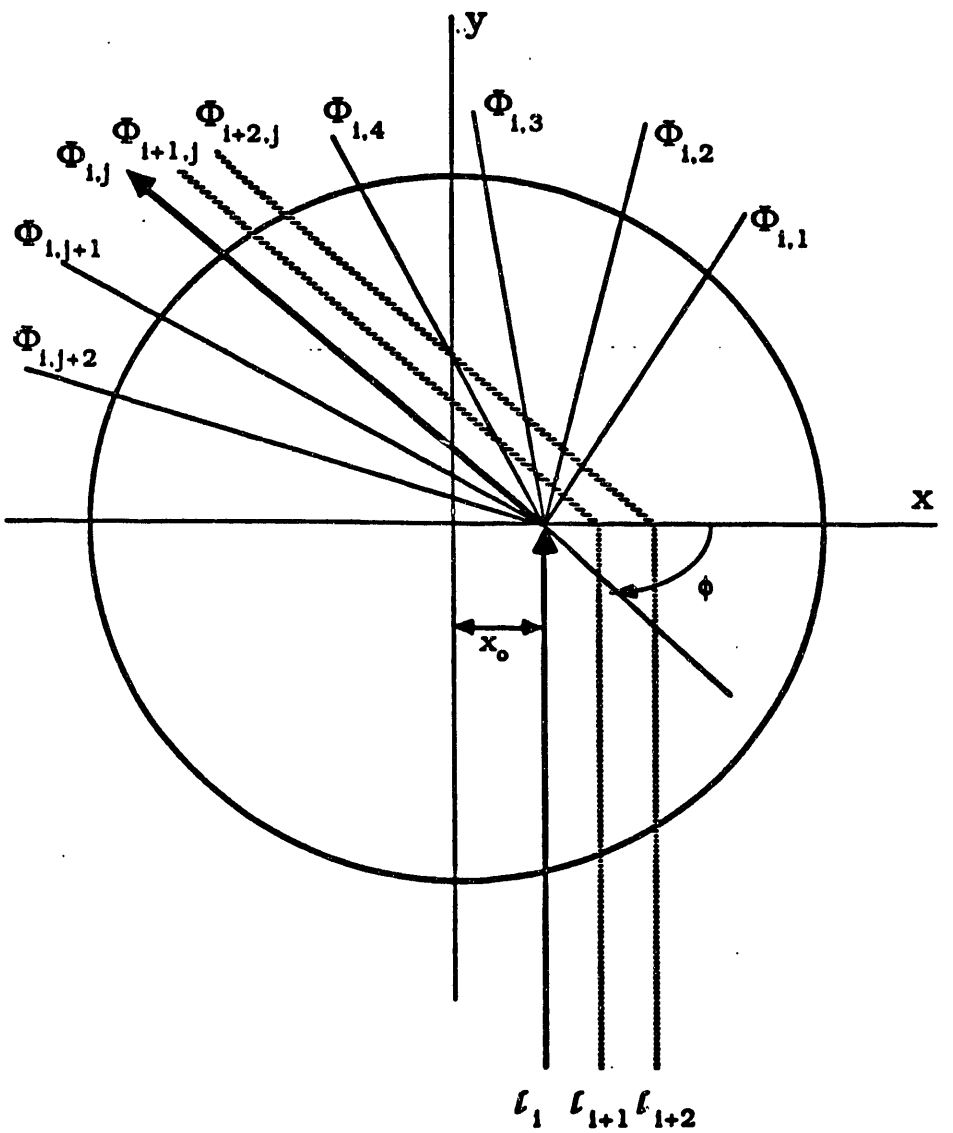

Fig.5 Nomenclature for angular tomography algorithm.

Then, Eq. (15) becomes

$$f(r,\Psi) = \int_0^{\pi} h[r\cos(\Psi-\Phi),\Phi]\,d\Phi \tag{17}$$

Fourier inversion of Eq. (13) is

$$P(l,\phi) = \int_{-\infty}^{\infty} F(R,\Phi)\exp(-2\pi i R l)\,dR \tag{18}$$

Note that the Fourier transform of $P(l,\phi)$ is $F(R, \Phi)$, and the Fourier transform of $h(l,\Phi)$ is $|R|$ $F(R,\Phi)$. Therefore,

$$\left[\text{FT of } h(l,\Phi)\right] \equiv \left[\text{FT of } P(l,\Phi)\right] \times \left[\text{FT of } q(l)\right] \tag{19}$$

if $|R|$ is the Fourier transform of $q(l)$, such as

$$|R| = \int_{-\infty}^{\infty} q(l)\,\exp(2\pi i R l)\,dl \tag{20}$$

Now, if we use the convolution relation of the Fourier transform, we write

$$h(l,\Phi) = \int_{-\infty}^{\infty} P(l',\phi)\,q(l-l')\,dl' \tag{21}$$

This means that we have to know the explicit form of the q-function to evaluate h-functions. The inverse Fourier transform of Eq. (20) is

$$q(l) = \int_{-\infty}^{\infty} |R|\,\exp(-2\pi i R l)\,dR \tag{22}$$

or, if we write the integral over a finite range of $\left(-\frac{A}{2}, \frac{A}{2}\right)$

$$q(l)\;\; q_A(l) = \int_{\frac{-A}{2}}^{\frac{A}{2}} |R|\,\exp(-2\pi i R l)\,dR \tag{23}$$

We can evaluate this integral explicitly, if we assume that $l = ma$ where m is either a positive or a

negative integer, and "a" is the distance between discrete measurements ($a \equiv \Delta l$). Eq. (23) can be evaluated to get

$$q(ma) = \begin{cases} \dfrac{1}{4a^2} & \text{for } m = 0 \\ \dfrac{-1}{\pi^2 m^2 a^2} & \text{for odd } m \\ 0 & \text{for even } m \end{cases} \tag{24}$$

We can rewrite Eq. (21) as

$$h(na,\Phi) = a \sum_{m=-\infty}^{\infty} P(ma,\Phi)\, q[(m-n)a] \tag{25}$$

or

$$h(na,\Phi) = \frac{P(na,\Phi)}{4a} - \frac{1}{a\pi^2} \sum_{\pm j,\,odd} P\left[(n+j)a;\Phi\right]\frac{1}{j^2} \tag{26}$$

which is to be used in calculating $f(r, \Psi)$

$$f(r,\Psi) = f(j r_0, k\Psi_0) = \frac{\pi}{N} \sum_{t=1}^{N} h\left[j r_0 \left|\cos(k\Psi_0 - t\Phi_0)\right|, t\Phi_0\right] \tag{27}$$

2.2.2 Application of Convolution Technique for Angular Tomography

After a long algebraic procedure (Menguc, 1988), we can use the expressions for computed tomography given above to obtain the $\bar{\beta}$-function which carries information about both the extinction and scattering coefficients and the phase function. For tomographic reconstruction of angular transmission/scattering data, we try to obtain the $\bar{\beta}$ function of Eq. (4). The modified form of the expressions read as

$$f = \bar{\beta} = \gamma^* + \beta^* \tag{28}$$

$$\gamma^* = \gamma\delta(\Delta s)\frac{1}{\Delta s} \; ; \qquad \gamma(x_0,\phi) = -\ln[\sigma(x_0)p(x_0,\phi)\frac{K}{4\pi}] \tag{29}$$

and

$$\beta^* = \begin{cases} \beta & \text{if } s \geq -s_0 \\ \beta dy/ds & \text{if } s < -s_0 \end{cases} \tag{30}$$

Once the f-function is determined, β and γ functions can be evaluated numerically, which will lead to scattering coefficient and phase function. A simple approximation for the phase function will be discussed in Section 2.4.

2.3 Inverse Monte Carlo Technique for Plane-Parallel Media

In addition to tomographic reconstruction technique, we also attempted to develop an inverse Monte-Carlo technique for determining the radiative properties of plane-parallel or axisymmetric cylindrical media. This technique will be extended to cylindrical geometry, and also it will be used to evaluate the other inverse schemes for a given geometry. Here, we do not give any mathematical details of the technique, and only present two tabular comparisons of results to show its applicability. More results will be presented in the next report.

In Table 1, the exact and predicted single scattering albedo values are compared for a single-layer, uniform plane-parallel medium. It is assumed that the scattering is isotropic. This is however, not a very restrictive approximation, because scaling of phase function using a delta-Eddington phase function would yield the same form of the equations. The inversion scheme is based on the measurements of transmission and reflection of incident light beam by the layer. (Note that, in tables, reflection is referred to as "albedo"). In this case, we assume that either 10,000 or 20,000 photons are emitted from the light source, and upto eight internal scattering in the medium is accounted for. As seen from the comparisons given, the inverse Monte-Carlo model is capable of predicting the exact single scattering albedo value of 0.8 within 10% error margin.

In Table 2, we compared the exact and predicted single scattering albedo values of each layer of a medium comprised of two uniform layers. We can extend the number of layers to any finite value to model property variations in a planar medium, although the computer time required will be excessive. Here, we assume that 40,000 photons are emitted from the light source, and we account for upto 10 internal scattering. Comparisons against the exact ω values (given in brackets)

Table 1 Inverse Monte Carlo predictions of single scattering albedo (omega) for a single, uniform layer cloud. (Exact values are shown in brackets).

FOR THE VALUE OF ALBEDO 0.2802
TRANSMISSION 0.4162
NO. OF PARTICLES 10000
MAX. SCATTERS 8

RUN	SEED	OMEGA ALBEDO	OMEGA TRANSM	PARTICLES ESCAPING
1	12345	0.8042	0.8001	9577
2	23456	0.8048	0.8095	9602
3	34567	0.8105	0.8101	9567
4	45678	0.8112	0.8007	9599
5	56789	0.8049	0.8042	9635
		(0.8)	(0.8)	

FOR THE VALUE OF ALBEDO 0.2802
TRANSMISSION 0.4162
NO. OF PARTICLES 20000
MAX. SCATTERS 8

RUN	SEED	OMEGA ALBEDO	OMEGA TRANSM	PARTICLES ESCAPING
1	12345	0.8002	0.7999	19688
2	23456	0.8014	0.8009	19700
3	34567	0.8028	0.8014	19668
4	45678	0.8087	0.7962	19692
5	56789	0.8018	0.8048	19693
		(0.8)	(0.8)	

Table 2 Inverse Monte Carlo predictions of single scattering albedo (omega) in each of two uniform parallel layers. (Exact values are shown in brackets).

****
****
NO. OF PARTICLES 40000
MAX. SCATTERS 10
****
****

FOR THE VALUE OF ALBEDO 0.0439
AND TRANSMISSION 0.2463

RUN	SEED	OMEGA LAYER1	OMEGA LAYER2	PARTICLES REMAINING
1	12345	0.199	0.205	239
2	23456	0.198	0.205	231
3	34567	0.199	0.201	236
4	45678	0.204	0.187	254
5	56789	0.193	0.226	259
		(0.2)	(0.2)	

FOR THE VALUE OF ALBEDO 0.0753
AND TRANSMISSION 0.3134

RUN	SEED	OMEGA LAYER1	OMEGA LAYER2	PARTICLES REMAINING
1	12345	0.201	0.795	239
2	23456	0.197	0.805	231
3	34567	0.198	0.801	236
4	45678	0.212	0.775	254
5	56789	0.197	0.805	259
		(0.2)	(0.8)	

FOR THE VALUE OF ALBEDO 0.0570
AND TRANSMISSION 0.2738

RUN	SEED	OMEGA LAYER1	OMEGA LAYER2	PARTICLES REMAINING
1	12345	0.200	0.499	239
2	23456	0.197	0.505	231
3	34567	0.199	0.500	236
4	45678	0.208	0.479	254
5	56789	0.194	0.516	259
		(0.2)	(0.5)	

FOR THE VALUE OF ALBEDO 0.2184
AND TRANSMISSION 0.3134

RUN	SEED	OMEGA LAYER1	OMEGA LAYER2	PARTICLES REMAINING
1	12345	0.793	0.215	239
2	23456	0.794	0.215	231
3	34567	0.798	0.205	236
4	45678	0.808	0.175	254
5	56789	0.791	0.228	259
		(0.8)	(0.2)	

show that, the agreement is very good for all four configurations considered. If we take the average of five or more predictions obtained with different seeds (random numbers) the accuracy would be improved even further. In general, using the Monte Carlo technique, we can predict single scattering albedo within 10% accuracy, for both single or multiple layer geometries. The model is also capable of reconstructing the albedo-phase function profile if the data are obtained at several oblique angles. In order to use with these type inversion schemes, we proposed a new step-Eddington phase function approximation, which is discussed in the next section.

2.4 Scattering Phase Function Approximations

It is very well known that coal particles scatter light highly anisotropically (Viskanta and Menguc, 1987). In order to model the radiative heat transfer in coal-fired systems, the scattering phase function is to be modeled accurately. It is usually difficult to consider the phase function obtained from the Lorenz-Mie theory, and it is preferable to expand it in a series in terms of Legendre polynomials. For highly forward scattering particles, however, it is not uncommon to require more than 100 terms in the series to express the phase function. Because of this, we need to introduce some approximations to the phase function, and these approximate models should be compatible with the solution models of the radiative transfer equation.

For the solution of the inverse radiation problem, we also need simple expressions of the phase function. Otherwise, the governing equations from which we are required to obtain the radiative properties become too cumbersome.

The scattering phase function can be written as

$$\Phi_\lambda(\Theta) = \sum_{n=0}^{N} a_{n,\lambda} P_n(\Theta) \tag{31}$$

where

$$a_{n,\lambda} = \frac{1}{2n+1} \int_{\Omega=4\pi} \Phi_\lambda(\Theta) P_n(\Theta) d\Omega \tag{32}$$

Here, Θ is the scattering angle, that is the angle between the incident beam and the scattered

beam. It is also possible to simplify the phase function by using a Dirac-delta function approximation (Crosbie and Davidson, 1985)

$$\Phi_\lambda(\Theta) = 2f\delta(1-\cos(\Theta)) + (1-f)\Phi_\lambda' \tag{33}$$

where

$$\Phi_\lambda'(\Theta) = \sum_{n=0}^{N} a'_{n,\lambda} P_n(\Theta) \tag{34}$$

Here, Φ'_λ is the normalized phase function with the forward peak removed, and δ is the Dirac-delta function. It was shown by Crosbie and Davidson (1985) that this functional representation is very effective for large water droplets ($x>100$) except in the forward scattering direction. However, it is not possible to use this expression to obtain the phase function from experiments, because of the delta-function.

Recently, we developed a step-Eddington phase function approximation to use along with experiments.

$$\Phi_{s-E} = 2fH(\cos\epsilon - \cos\Delta\Theta) + (1-f')\sum_{l=0}^{K} A_l' P_l(\cos\Theta) \tag{35}$$

where, H is the Heavyside function, and $\Delta\Theta$ is the angular step in the forward direction. This approximation has been used first time and the details will be given in an upcoming paper (to be submitted to Applied Optics, Menguc and Subramaniam, 1988).

In Figs. 6 and 7, the reconstructed delta-Eddington and step-Eddington phase functions are compared against the "exact" results obtained from the Lorenz-Mie theory. Two different complex index of refraction used in these results, i.e., in Fig.6 n=1.85-i0.04, and in Fig.7 n=1.80-i0.04. It is assumed that the scattering of CO_2-laser (λ = 10.6 μm) by the medium is recorded at 10 angles, and there is a random $\pm$ 10% experimental error at all angles, except the forward direction, at which error is 25%. In general, good agreement is observed between the predictions and the true values. The step-Eddington approximation was capable of predicting the forward peak accurately; however, neither of the models could follow the fluctuations observed in true phase function. This is not a significant drawback for practical applications, where a size distribution of particles is to

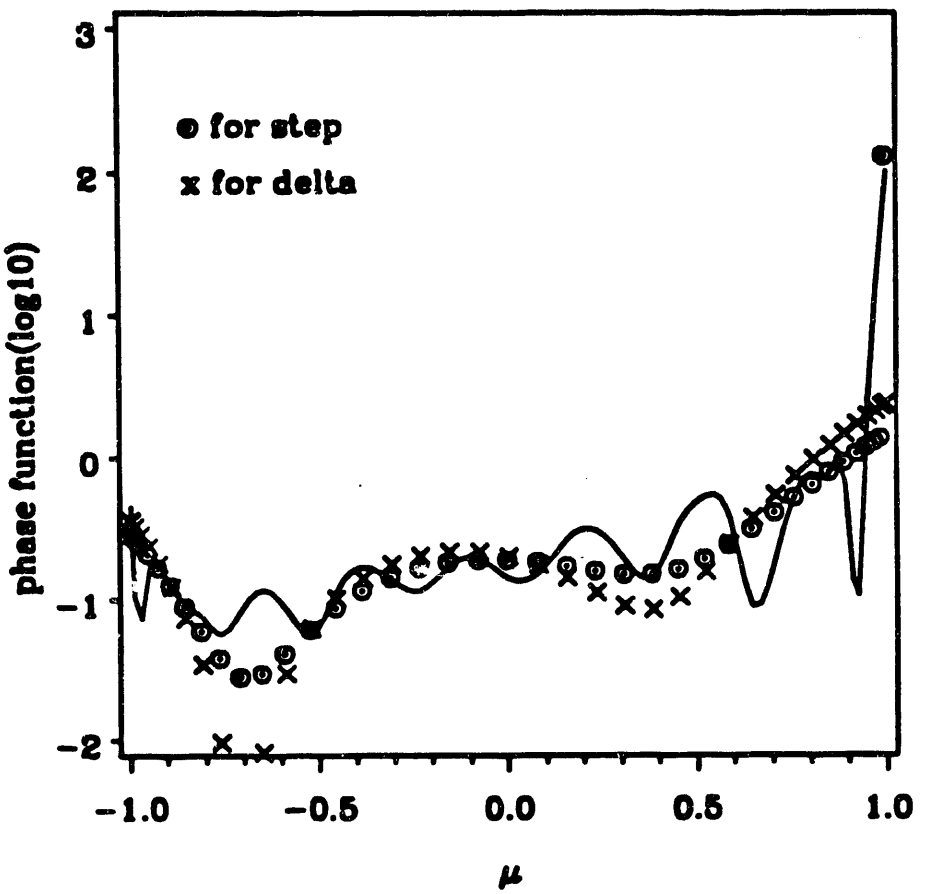

Fig.6 **Phase function for coal, n=1.85+0.04i, with x=10.0,λ=10.6 , dia.=33.24 (in μm) from 10 obs. with +25% error in p(0) value and −10 to +10% random error in others. Reduced to 4 term step and delta fns. from coeff. of step fn. approximation**

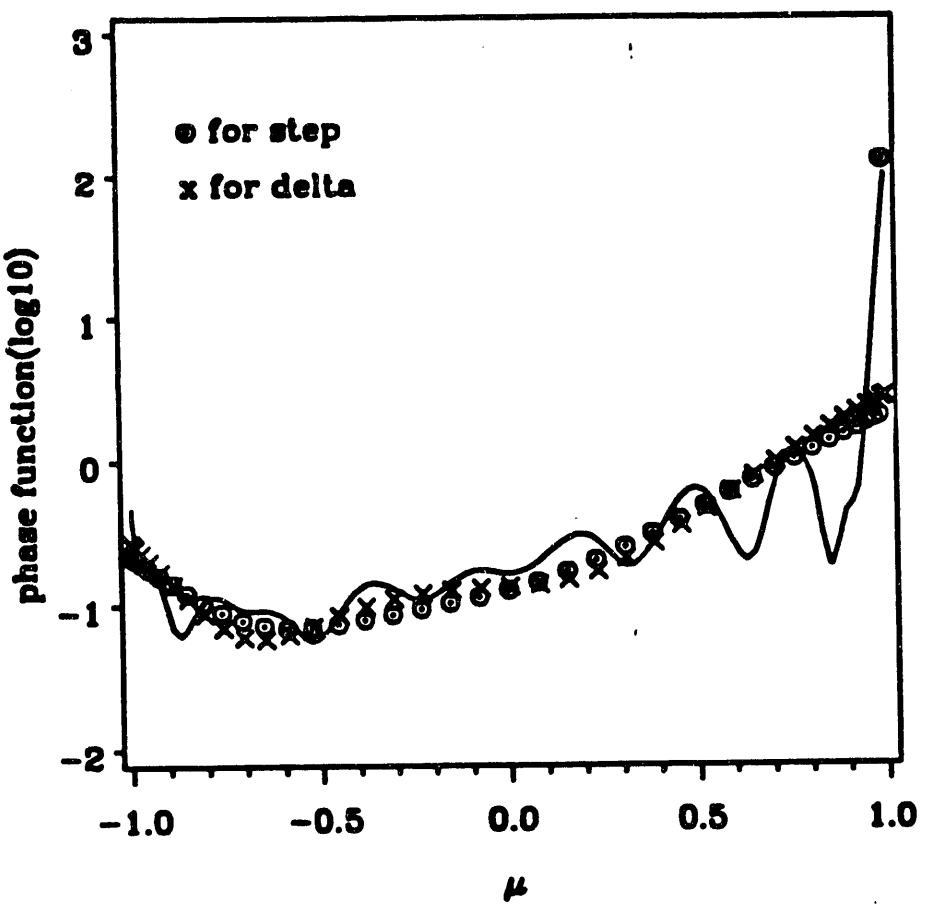

Fig.7 **Phase function for coal, n=1.50+0.04i, with x=10.0,λ=10.6 , dia.=33.24 (in μm) from 10 obs. with +25% error in p(0) value and −10 to +10% random error in others. Reduced to 5 term step and delta fns. from coeff. of step fn. approximation**

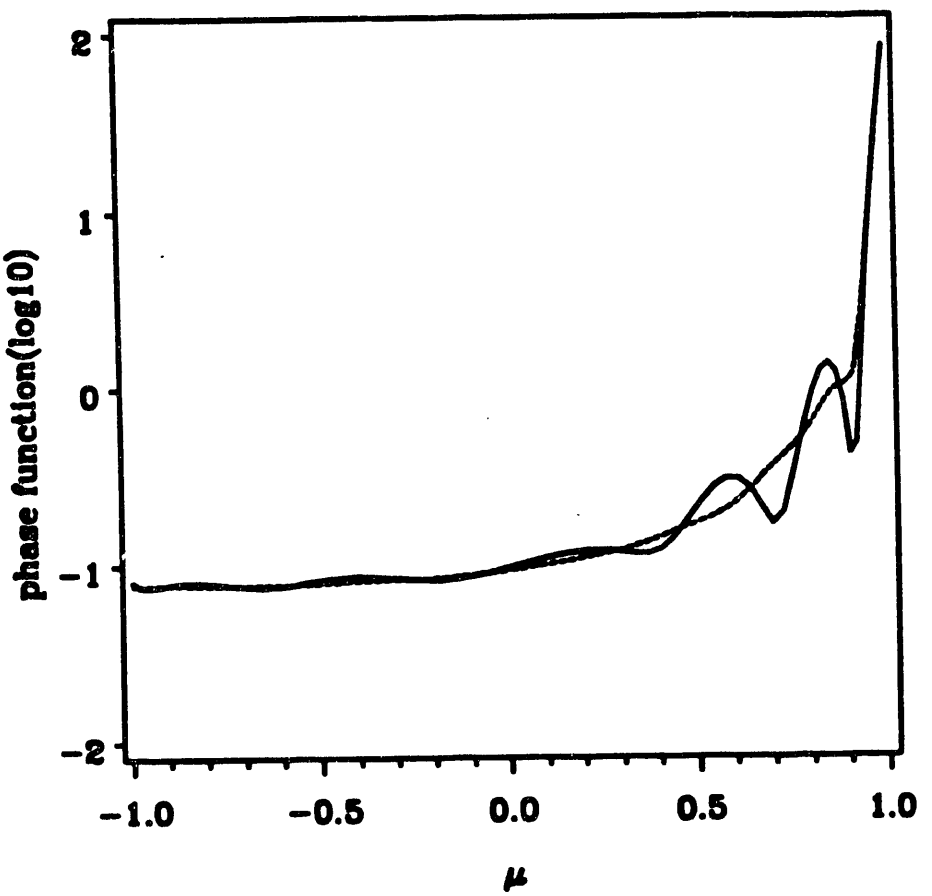

Fig.8 **Phase function for coal, n=1.85+0.22i, with λ=10.6 , dia.=20–35 (both in μm) plotted vs. the phase fn. for dia. =27.5 (equal weights for dia=20.5–34.5 (15dia.))**

be used, and because of this most fluctuations will be smoothed out. In order to test the effect of a size distribution on results, the step-Eddington approximation is obtained using the "numerical" measurements of an arbitrary phase function at 10 angles. The test phase function is calculated from the Lorenz-Mie theory for an equal-weight size distribution of particles of diameter 20-35 μm at λ=10.6μm (CO_2-laser wavelength). The comparison of the true and predicted step-Eddington phase functions are depicted in Fig.8. It is clear that agreement here is good and the simple approximation looks promising for future application to coal-flame experiments.

3 EXPERIMENTAL STUDIES

As we mentioned earlier, determining the local radiative properties of a medium by solving the inverse radiation problem requires some knowledge about the scattering of light by the medium. In this section, we will review some of the experiments in scattering of light and discuss how they could be useful to the problem under consideration. In most of the experiments discussed below, laser radiation is used as the incident light.

3.1 Experiments in Light Scattering - A Literature Review

An early effort in this field is that of Atkins (1965). He used injection molded solid plastic disks about 4 cm in diameter and 1 mm thick for his scattering medium. He found that for small values of optical thickness the problem becomes two dimensional because radiation gets scattered out from the edges of the disks. He obtained good comparison between theory and experiment if the dye absorption coefficient and the magnitude of the scattering phase function were adjusted.

Hottel et al. (1968) demonstrated the importance of considering Fresnel reflection at the interface of a slab containing isotropic or anisotropic scatterers. They showed that interface reflection causes a significant decrease in the magnitude of both reflectance and transmittance and a marked alteration in the angular distribution of the energy reflected and transmitted by the slab.

Sarofim et al. (1968) studied the angular distribution of scattered radiation by 3.49 μm polyvinyl toluene spheres closely packed in a monolayer. The size parameter was varied by changing the

wavelength, and the experiments performed showed that intensities within the range of angles in which the diffraction pattern provides the major contribution to scatter (0-20°) are considerably lower than that calculated by theory.

Hottel et al. (1970) examined the validity of the assumption about neglecting polarization effects when dealing with the solution of the transport equation for scattering media. Their experiments showed that radiative properties of the uniformly distributed particles in suspension may be calculated with confidence from the Lorenz-Mie theory. They also found that polarization effects could be neglected.

In another work, Hottel et al. (1971) derived a correlation for the effect of interparticle spacing on the scattering cross section for monodisperse matrix-suspended pigment particles. The particles were spheres of diameter from 0.102 to 0.530 μm, and they were non-absorbing with effective refractive index of 1.20. The correlation they derived shows that for pigment suspensions that can be described as an assembly of Mie scatterers the optical properties can be calculated from pure theory with no empirical constants.

Querfield et al. (1972) measured bidirectional transmission of uniform polystyrene latex spheres in distilled water. They investigated a polystyrene latex of narrow size distribution and of the average diameter 0.245 μm. The incidence of the radiation was varied from 0 to 36.0° from the normal. The experiments compared well with theory and, in fact, the experimental arrangement can serve as an analog computer for other systems for which the theory is too complex for machine calculations.

Margolis et al. (1972) studied the reflection in the normal direction by uniform polystyrene latex spheres (n= 1.1943) in distilled water. The measurements were made in the multiple scattering regime of the diffuse reflectivity as a function of single scattering albedo. The experimental methods and techniques used by the authors provide a sensitive way of measuring small but not negligible particle absorption. Particles of diameter 1.10 μm and 0.109 μm were used.

Granatstein et al. (1972) performed a controlled laboratory experiment to study the reflectance of turbid water as a function of the absorber and scatterer concentrations. Laser light was incident

on water containing two types of materials, one that scatters light (teflon particles) and one that absorbs light (black dye). The size of the particles was in the Mie theory region ($0.264 < x < 2.64$), and the experiments agreed closely with appropriate solutions from the radiative transport equation.

Howard and Novotny (1974) used (probably for the first time) polydispersed, nonspherical titanium-dioxide particles in glycerol. They studied the bidirectional reflection of the particles of size parameter equal to 1.75 and 2.33 . Their results agreed closely with those obtained from theory.

Leader and Dalton (1975) performed a series of experiments to determine the effects of changes in single scattering albedo and optical thickness of a scattering medium of latex spheres (x=0.54 and n=1.194) on the measured scattering cross section and its angular distribution. The experiments compared well with theory for optical thicknesses of 1.0 and 10.0, but discrepancies were observed for optical thickness of 0.1.

Janzen's work (1980) confronts the question regarding the choice of the diameter for an optically equivalent sphere in the case of irregularly shaped particles. He used carbon blacks of various types ($1.72 \leq n \leq 2.13$; $0.16 \leq x \leq 3.0$) and showed that despite serious nonsphericity of the particle entities involved, observed extinction spectra for dilute carbon black sols are fitted precisely by the Mie theory for ensembles of spheres. These spheres must be quite nearly volume equivalent to the actual colloidal carbon units.

Incropera et al. (1981) studied the directional and spatial distributions of the spectral radiation in a diffusely radiated aqueous medium. The medium was characterized by an extinction coefficient of 0.089 cm^{-1}. and albedo of 0.72. A plexiglas tank was used as an experimental cell, and 12 150-W flood lamps were used as light sources. The results obtained from the experiments compared favorably with the solutions obtained using the discrete ordinates and three flux methods.

The attenuation constant of a coherent field in a dense distribution of particles was measured by Ishimaru and Kuga (1982). They studied the effect of the pair-correlated distribution of scatterers on the propagation characteristics of the coherent field. They showed that for particle density

greater than about 0.1 %, the attenuation constant departs markedly from the formula based on an uncorrelated scattering assumption. It decreases sharply when $x<1$ and shows a slight increase when $x>>1$. They assumed an effective diameter in the particle diameter for the particle distribution that gave the value of the ratio of measured to the experimental value of the attenuation constant to be unity.

Look et al. (1981) studied the anisotropic scattering from a semi-infinite medium exposed to a laser beam. A suspension of latex particles ($0.26<x<25$) was used as the medium. The laser beam was incident normal to the purely scattering medium and the back scattered radiation was predicted as a function of the distance from the beam. The experiments showed that the influence of anisotropic scattering shifts the maximum of the radial distribution of the scattered intensity to larger optical radii as the particle size increases.

Brewster and Tien (1982) examined the radiative transfer in packed fluidized beds. They used 11.0 μm diameter latex particles and a He-Ne laser as the light source. Their experiments showed that interparticle spacing measured in terms of the wavelength is the most critical parameter to gauge the importance of dependent scattering and that high particle concentration alone is no indication that scattering is dependent.

Craig and Incropera (1984) have made radiation measurements in highly scattering and absorbing aqueous suspensions. They used India ink particles (0.02 μm-0.06 μm) and powdered talc particles (15-40 μm). The probes used in the experiment determined the vertical and directional distributions of the radiance as well as the vertical distribution of the downward flux. The experiments revealed the effect of the suspension opacity, scattering albedo and bottom reflectivity on the radiation field.

Nelson et al. (1986) extended the results obtained by Look et al. (1981) to the optically thick region. They showed that the back scattered radiation in optically thick media is very sensitive to changes in the scattering albedo, especially when the albedo is close to 1 .

Tien et al. (1986) worked on the same apparatus as Brewster and Tien (1982) and studied the dependent scattering by particles. They used plane parallel cells containing latex spheres of 0.08,

2, and 11 μm diameter dispersed in an air or water matrix. They found that close packed 2 μm particles did not show dependent scattering. For the 0.08 μm particles, the scattering efficiencies decrease as volume fraction increases.

Kamiuto and Iwamoto (1987) developed a method to study the combined conductive and radiative heat transfer through a glass particle layer. The mean diameter of the soda-lime-silica glass particles was taken as 0.00167 m. They determined the temperature profiles and heat transfer characteristics of the particle layer.

A method for measuring the radiative properties of a fibrous porous medium was developed by Kurosaki et al. (1987). They used the apparent emissivity of the porous medium and the inverse method to determine properties such as the extinction coefficient, the scattering albedo, and the back scattering fraction factor. The values found for commercial glass agreed well with earlier experimental values available in the literature.

Lately, Boothroyd et al. (1987) made measurements of the light scattering phase functions and asymmetry factors for a sample of fly ash particles. The average size parameter was close to 33. Their results showed that fly ash can be treated as spherical particles under furnace conditions where they are well dispersed.

These experiments are compared tabularly for easy cross-reference.

3.2 Pulverized-Coal Flow Experiments

Our main goal is to determine the radiative properties of coal particles as they are. It means that all surface irregularities, size distribution effects, and complex index of refraction uncertainties should be buried in the effective models we are developing. In order to adopt an experimental strategy to serve this purpose best, we divide the experiments in two categories:

i) Simple non-flame experiments;

ii) Flame experiments.

EXPERIMENTS IN RADIATION

Year	Reference	Scattering Medium	Property Measured	Character of Medium	Parameters Investigated	Major Findings
1961	Dezelic and Kratohvil	Uniform polystyrene latex spheres in distilled water	Transmission, Polarization ratio, dissymmetry, angular scattering	$1.199<n<1.214$ $0.48<x<9.09$	θ, $P(\theta)$, x	Mie theory can be applied applied to the light scattering of latex particles. Measurements give diameters lower than those from electron microscopy.
1964	Woodward	Uniform polystyrene latex spheres in distilled water	Angular scattered intensity	$n=1.2$ $x=22.2, 16.5$	x, τ	The Hartel multiple scattering theory is verified experimentally using fairly high concentration of spherical latex particles.
1965	Atkins	Polydispersed rutile titanium dioxide spheres and dye in plastic discs	Transmission and Reflection	$x = 1.54$ $n = 1.87$	τ_o, ω	Good comparison between theory and experiment if dye absorption and magnitude of scattering phase function adjusted.
1965	Kratohvil and Smart	Uniform polystyrene latex spheres in distilled water	Absolute angular scattered intensity	$n=1.199$ $x=8$ to 12	p^* and effect of solid angle	Polarization effects are not important. Reflections from cell wall must be accounted for.
1965	Smart, Jacobsen, Kerker, Kratohvil & Matijevic	Polystyrene latex spheres	Multiple scattering	$n=1.194$ $x=7.35; 9.2$	θ, τ, x	Experimental results for multiple scattering matched closely with those obtained from the Hartel theory.
1968	Sarofim, Hottel and Fahimian	Uniform polyvinyl toluene spheres painted on a glass slide	Bidirectional transmission	$9.56<x<25.16$ $1.56<n<1.61$	θ, p^*, x	Particles can be treated as Mie scatterers except in a 20° cone in the direction of forward scattering.
1970	Hottel, Sarofim, Vasalos & Dalzell	Uniform polystyrene latex spheres in distilled water, 0.106 and 0.530 μm	Bidirectional transmission and reflection	$0.815<x<5.12$ $n=1.19$-1.20; $0.25<\tau_o<3000$	θ, p^*, x τ_o	For clearance $>0.3\ \lambda$, single scattering properties can be used for multiple scattering. Polarization effects can can be neglected.

Year	Reference	Scattering Medium	Property Measured	Character of Medium	Parameters Investigated	Major Findings
1971	Sarofim, Vasalos and Jeje	Uniform polystyrene latex spheres in distilled water	Bidirectional transmission and reflection	$x=1.90;2.38$ $n=1.20$ $0.20<\tau_o<2.0$	θ, x, τ_o ω	Good compansion between theory & experiment obtained by adjusting scattering particle diameter.
1971	Hottel, Sarofim, Dalzell & Vasalos	Uniform polystyrene latex spheres in distilled water	Bidirectional transmission and reflection	$0.764<x<3.05$ $1.14<n<1.20$ $0.01<\tau_o<3211$	θ, x, τ_o	A correlation is given to accomodate the variation in effective scattering cross sections of close packed media for clearance $>0.3\lambda$ and $>0.4d$.
1972	Querfield, Kerker & Kratohvil	Uniform polystyrene latex spheres in distilled water 0.245 μm	Bidirectional transmission	$x=1.875;2.348$ $n=1.194$ $0.05<\tau_o<1.2$	θ, p^*, x τ_o	Experimental arrangement can be used as an analog computer for systems for which theory is intractable.
1972	Margolis, McCleese and Hunt	Uniform polystyrene latex spheres in distilled water	Reflection in normal direction	$x=1.09;11.03$ $n=1.194$	x, τ_o, ω	Technique to study behavior of cloudy planetary atmospheres.
1972	Granatstein, Rhinewine, Levine, Feinstein, Mazurowski & Piech	Polydispersed teflon spheres in distilled water	Reflection at $\theta=24$ deg for $\theta in=24$ deg	$0.264<x<2.64$ $n=1.89+i.0002$	ω	Successful theoretical model for multiple scattering of light by a turbid medium.
1974	Howard & Novotny	Polydispersed non-spherical titanium-dioxide particles in glycerol	Bidirectional reflection	$x=1.75;2.33$ $n=1.90;2.03$	θ, τ_o	Bidirectional reflectance for titanium dioxide particles.
1975	Colby, Narducci, Bluemel & Baer	Uniform polystyrene latex spheres in distilled water	Angular irradiance distribution and irradiance correlation function	$n=1.199$ $x=2.06, 3.18, 5.24$	x, τ	Deviations from Mie pattern is obtained for dense suspensions. Relaxation time for multiple scattering much smaller than that obtained from single scattering model.
1975	Leader & Dalton	Uniform polystyrene latex spheres in distilled water	Reflection at $\theta=20$ deg for $\theta in=35$ deg	$x=0.54$ $n=1.194$	ω	Good comparison of theory with experiment for $\tau=1.0$ and 10.0. Discrepancies for $\tau=0.1$.

Year	Reference	Scattering Medium	Property Measured	Character of Medium	Parameters Investigated	Major Findings
1976	Pinnick, Carroll & Hofmann	Nonspherical particles of sodium chloride and potassium sulfate	Angular scattering	n=1.54;1.49 3<x<10	θ,p*	For x<5 results match Mie theory but for x>5 the light intensity is more in the forward scattering lobe and less at other angles as compared to values from Mie theory.
1978	Look, Nelson, Crosbie & Dougherty	Latex paint in distilled water	Scattered intensity	Mixture of latex, titanium dioxide and pigment	τ	The intensity leaving the media can be expressed as a function of the optical radius.
1980	Janzen	Carbon blacks	Dimensionless Optical Density Spectra	1.72≤n≤2.13 0.16≤x≤3	λ,c	Extinction spectra for dilute carbon black sols are fitted precisely by Mie theory for ensembles of sphere.
1981	Incropera, Wagner & Houf	River Water	Directional & spatial distribution of the spectral radiation	ω_λ=0.72 β_λ=0.089/cm	θ,τ	Good comparison of experimental results with those obtained from discrete ordinante and three flux methods.
1981	Ishimaru & Kuga	Latex spheres in water solution	Attenuation constant of a coherent field	0.529<x<82.80 n=1.17 to 1.19	fv,c	Attenuation constant decreases sharply when x<1 and increases slightly when x>>1.
1981	Look, Nelson & Crosbie	Latex particles in a water solution	Back scattered radiation	0.1<τ_o<10 0.26<x<25 n=1.20	θ,τ_o	Influence of anisotropic scattering shifts the maximum of the radial distribution of scattered intensity to larger optical radii as the particle size increases.
1982	Brewster & Tien	Suspension of latex particles	Transmittance and Reflectance	f_v=0.01-0.7 (close packed)	θ,c/λ	Inter-particle spacing measured in wavelengths is the most critical parameter to gauge importance of dependent scattering.

Year	Reference	Scattering Medium	Property Measured	Character of Medium	Parameters Investigated	Major Findings
1984	Incropera & Craig	Aqueous suspension of India ink and powdered talc	Intensity & Flux	Ink:0.02-0.06μ ω<0.20 Talc:15.40μ ω>0.80 1<c<15	θ,z	The effect of the suspension capacity, albedo and bottom reflection on the radiation field.
1986	Nelson, Look & Crosbie	Latex particles in a water solution	Back scattered radiation	0.3<x<2.31 n=1.195	τ_o,ω $P(\theta)$	Back scattered radiation in optically thick media is very sensitive to changes in ω, when ω is near 1.
1986	Tien, Yamada & Cartigny	Polydivinylbenzene spheres Polyvinyltoluene " Polystyrene sphere in air/water	Dependent scattering efficiencies. Bidirectional Reflectance & Transmittance	x=0.529,14.4 79.3 n=1.19	f_v,θ τ	Closed packed 2μm particles didn't show dependent scattering. For 0.08 μm particles dependent scattering efficiencies decrease as volume fraction increases.
1987	Kamiuto & Iwamoto	Glass particles (spheres)	Temperature profiles, and conductivity	mean dia 1.67×10^{-3} m No. density $231.5\times10^{6}/m^3$ $226.2\times10^{6}/m^3$	ω,g	Analytical method is useful to predict the temperature profiles and heat transfer characteristics of a layer of glass particles.
1987	Kurosaki Take-uchi, Kashiwagi, & Yamada	Fibre Glass (plane porous medium)	Apparent emissivity	L=1.05×10^{-3}m w(kg/m^2)= 3.0×10^{-2} d(μm)=15.5 fv=0.0112	ω,β,b	Method using apparent emissivity of a porous medium and inverse method is useful to determine radiative properties of a fibrous porous medium.
1987	Boothroyd, Jones, Nicholson, & Wood	Fly ash particles	Intensity	n=1.5-i0.012 $x_{mean} \approx 33$	$P(\theta)$	Fly ash can be treated as spherical particles under furnace conditions.

Year	Reference	Scattering Medium	Property Measured	Character of Medium	Parameters Investigated	Major Findings
1987	Drolen, Kumar & Tien	Latex particles in a water solution	Dependent scattering cross sections	$x=0.0205$ $f_v=0.001$ to 0.12	f_v	Verified the criterion of $f_v=0.0064$ for $x<0.4$ as a lower limit for dependent scattering.
1987	Nelson & Satish	Uniform polystyrene latex spheres in distilled water	Transmission of laser beam through a multiple scattering medium	$n=1.194$ $x=3.18$	τ	The anisotropic scattering data correlates with scattering theory for optical thicknesses of 2.0-10.0.
1988	Chylek, Srivastava, Pinnick & Wang	Composite spheres of acrylic and water	Differential scattering cross section	$n=2\pi$ $\lvert n,x \rvert = 0.32$	$P(\theta)$,n	The experiments provide a test to various existing and future theoretical models for scattering by non-homogeneous particles.
1988	Nelson & Satish	Uniform polystyrene latex spheres in distilled water	Radial scattering	$n=1.197$ $x=0.601$, 3.178	τ,x	Single scattering approximation holds for optical depth up to 0.4 if depth-to-diameter ratio is unity.

Our current focus is on the simple non-flame experiments, which would give us an idea about our potential and accuracy in determining the radiative properties of coal particles without being affected by the hostile flame environment. For this, we decided to design an experimental test cell in which we can suspend coal particles of known rank, size, and size-distribution.

The short term goal of this experiment is to use transmission measurements at five different wavelengths to calculate the extinction efficiency of a one dimensional coal stream for different size distributions of coal particles.

3.2.1 Coal Test Cell Apparatus

Initially, our tests are focused upon working with a non-flame environment. A coal test cell was designed to create a near uniform flow of coal particles operating on the basis of gravity. A schematic of the coal test cell is shown in Fig. 9. It consists of a cylindrical section on top with a conical type section connected underneath. Coal is fed into the coal test cell by means of a fluidized bed coal feeder. As the flow of coal is started, it is fed upward into the cylindrical section of the coal test cell along with an extra flow of air. A "fountain-type" flow is created in the top of the test cell reducing the effect of a parabolic velocity profile. The additional air serves to distribute the coal in a more uniform flow field. As the air/coal mixture reaches the bottom of the cylindrical test section, it flows through an initial section of smoothing screens. This section contains a conical funnel above two screens of five openings per centimeter each. The funnel is necessary to prevent the accumulation of coal particles on the bottom cap of the cylindrical test section. Once the particles had accumulated, they tended to fall in irregular patterns causing the flow field to be nonuniform. Also, a mechanical vibrator was mounted on the side of the cylindrical test section just above the bottom cap. Figures of the voltage output operating with and without the vibrator show a significant difference in uniformity of the flow field.

At the exit of the cylindrical test section, the coal/air mixture enters into a conical type test section. The purpose of this design is to create a one dimensional flow field with a small optical path length (width) through the coal stream. Two smoothing screens of four openings per centimeter each are located twenty and twelve centimeters from the bottom of the test section. Two

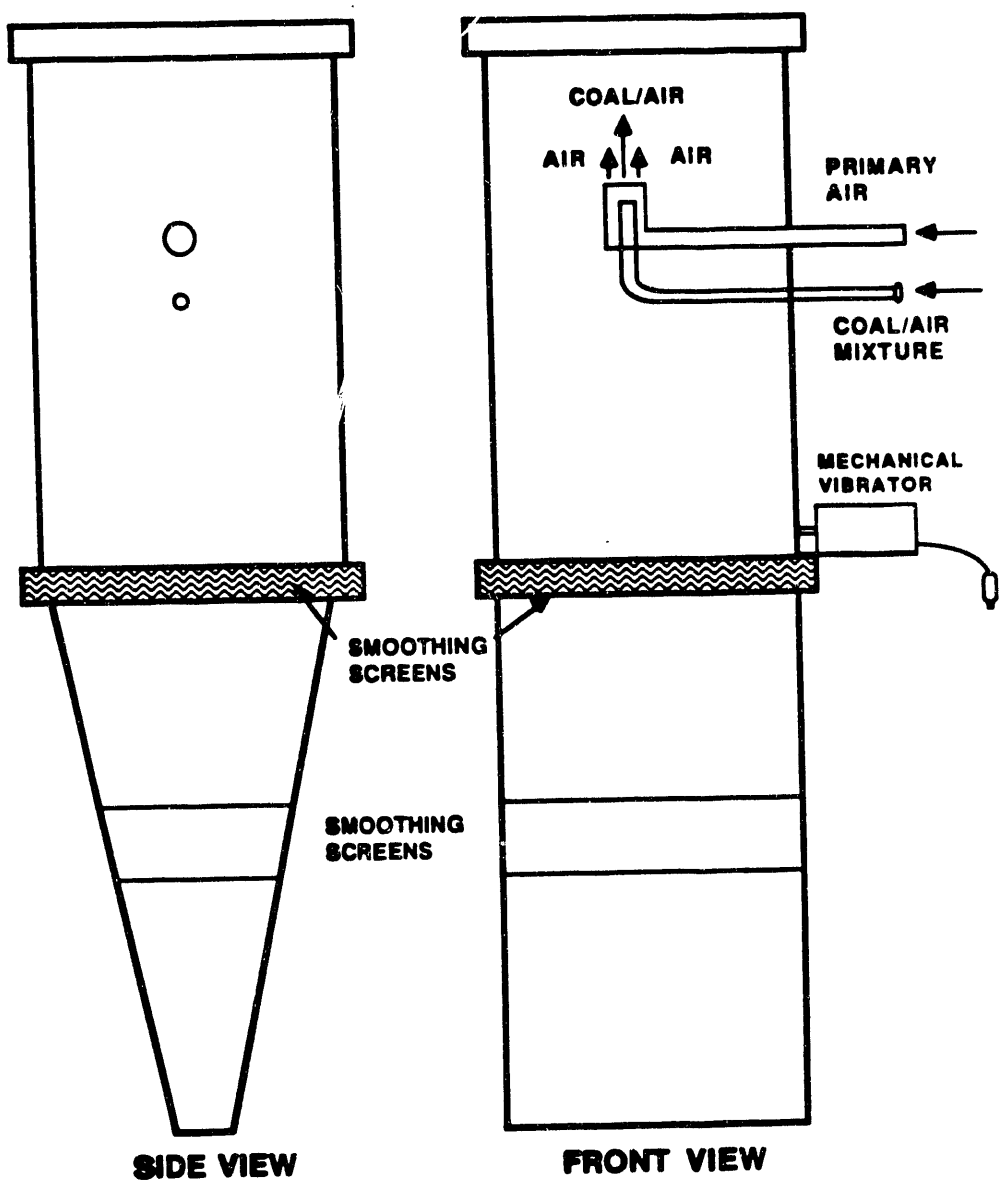

Fig.9 Test Cell for cold pulverized-coal s.ream experiments.

opposing air jets are located one centimeter below the last smoothing screen. This air flow serves to separate any particles that may have agglomerated in the flow field. At the bottom of the test section, there are front and rear extensions which decrease the optical path length of the one dimensional coal stream. A sliding coal gate is mounted on the bottom of the test cell. This provides a means of deflecting the coal stream around the radiation source beam so that the fluidized coal feeder can operate continuously throughout an experiment. A vacuum system is used to collect the coal once it passes through the test cell. The collected coal is stored for future reclassification.

3.2.2 Optical and Detection System

An infrared blackbody source, operating at 1273 K, is being used to project a narrow beam of broad-band radiation across a line of sight passing through the one dimensional coal stream just underneath the coal test cell. A schematic of the optical arrangement appears in Fig. 10. The beam is passed through a chopper, operating at a certain frequency which maximizes the detector signal and through two consecutive aperture stops of four millimeters each. The beam is focused onto the thin coal stream with a combination of a plane mirror and a spherical mirror having a focal length of 18.5 centimeters. The two aperture stops restrict the solid angle of the source beam to approximately 0.00034 sr.

The transmitted source beam is then refocused onto a detector using a combination of one spherical mirror and two plane mirrors, the prior having a focal length of approximately 15 centimeters. The optical thickness of the one dimensional coal stream was sufficiently small so that acceptance into the line-of-sight of forward-scattered radiation can be considered negligible. Each of the five detectors used received sequential information by rotating one of the plane mirrors with a gearing system. This provided for very accurate positioning of the source beam.

A similar four-wavelength pyrometer has been used to measure particle and gas temperatures in one-dimensional, pulverized coal/oxidizer flames stabilized on a specially designed, flat-flame burner (Mackowski, 1986). Five infrared detectors, each coated with a narrow band interference filter, are being used at wavelengths of 0.8, 1.0, 2.3, 2.7, and 3.8 μm. Silicon detectors are used for

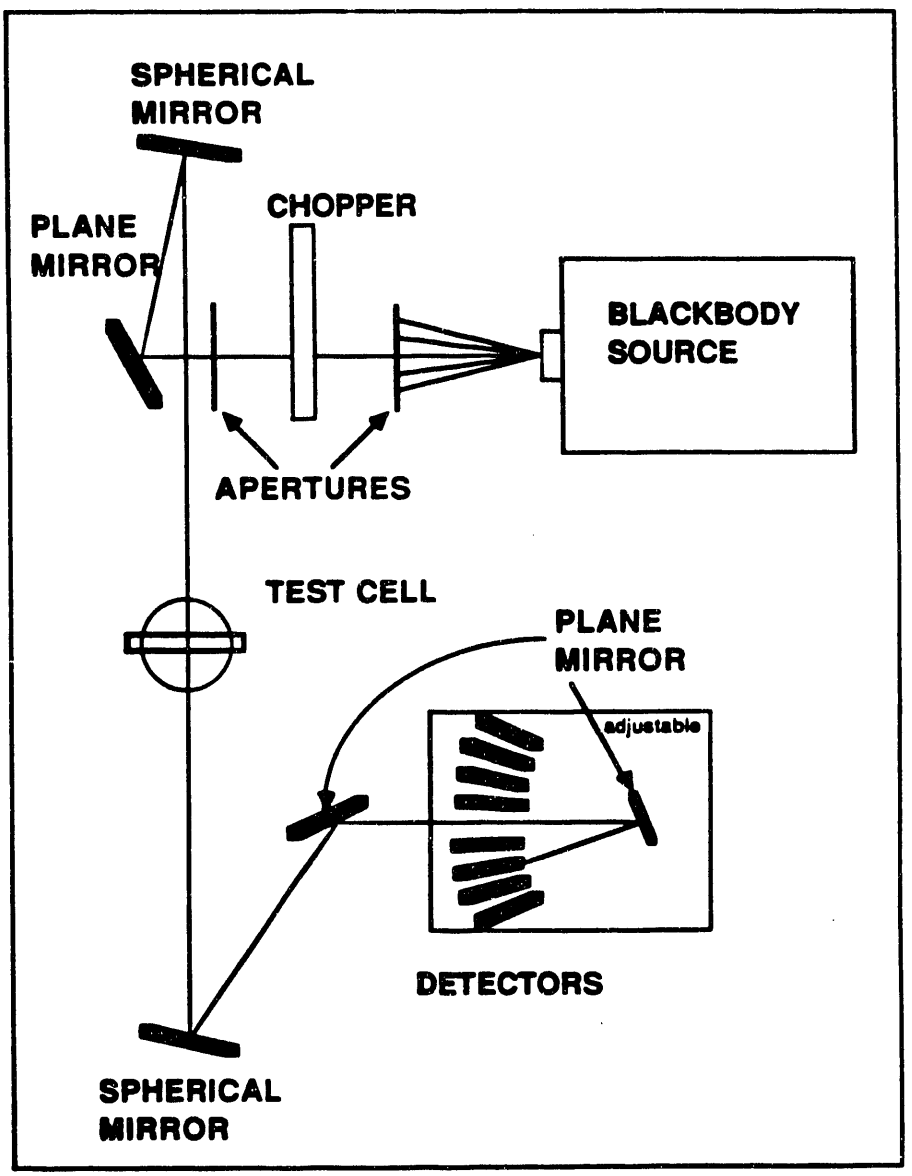

Fig.10 Optical system configuration for coal-stream experiments.

0.8 and 1.0 μm (Infrared Industries (IRI) model 1000), lead sulfide detectors for 2.3 and 2.7 μm (IRI 2600), and a lead selenide detector for 3.8 μm (IRI 5600). The lead sulfide and lead selenide detectors are thermoelectrically cooled for enhanced sensitivity. A lead selenide detector for 4.4 μm (IRI 5600) will be utilized later in the flame experiments. The 4.4 μm detector is within the fundamental CO_2 vibration band, along with the 2.7 μm detector which is sensitive to water vapor radiation, is used to measure the combined gas/particle cloud transmission. Knowledge of the particle cloud properties from the particle wavelength measurements of the other detectors allows the calculation of the gas temperature from the data measured at 2.7 and 4.4 μm.

The electrical signals generated by the detectors are linear to the radiant intensity of the black-body source. They are fed into a signal amplifier and then into a 14 channel analog tape recorder/reproducer (Kyowa RTP-600) where they can be recorded for later analysis. The voltage output from the tape deck is amplified to a range of 500 to 1500 mV, depending upon the detector sensitivity. The output from the tape deck is directed into a lock-in amplifier which is referenced to the chopper frequency, thus magnifying the signal-to-noise ratio.

A data acquisition system utilizing a 12 bit analog-to-digital converter (Data Translation Model DT-2801) installed in an IBM PC-XT is used to measure the signal from the lock-in amplifier. Simultaneous data sampling and averaging is controlled by a BASIC/8088 assembly code routine.

3.2.3 Experimental Procedure

To begin an experimental test run, the coal mass flow rate is adjusted to the desired level. It is monitored throughout the experiment on a strip chart recorder which provides a way of checking the consistency of the flow rate and also serves as a "hard-copy" output. All volumetric air flow rates and pressures are documented.

The source beam is directed onto the 0.8 μm detector and a measurement of the radiant intensity without the presence of a coal stream (V_o) is made by deflecting it with the sliding coal gate. Next, a measurement of the radiant intensity is made with the coal stream (V_t) by removing the coal slide gate. The time period for measurement of V_o and V_t is approximately 20 and 180

seconds, respectively. The source beam is then redirected onto the next detector and the measurement procedure is repeated. This method provides an accurate transmission measurement for each wavelength.

In Fig.11, the voltage readings for a typical experiment for different wavelengths are shown. The first part of the readings correspond to readings when there are no coal particles; the latter, lower values are for transmission through the pulverized-coal stream. The experimental data are very stable, as seen from these figures. Also, we average the readings over 2 to 3 minutes, to avoid the adverse effects of possible stray data points. The data reduction for these experiments are discussed in the next section.

3.2.4 Data Reduction

Because of the linearity of the detector output voltage with respect to radiant intensity, the transmissivity of the coal stream along the line-of-sight is given by $T=V_t/V_o$, where V_t and V_o are the detector voltages measured with and without the coal stream present, respectively.

The transmissivity is related to the optical thickness (β) by the relation,

$$T=\exp(-\beta L) \tag{36}$$

where β is the extinction coefficient (1/m), and L is the optical path length through coal stream (m) The extinction coefficient, neglecting the effect of the size distribution, is given by the following equation:

$$\beta = \frac{3}{2} Q_e f_v / D_p \tag{37}$$

where, Q_e is extinction efficiency factor, f_v is particle volume fraction, and D_p is effective spherical particle diameter.

The extinction efficiency is a function of the size parameter, which is given by $x = \pi D_p/\lambda$ where λ is the particular wavelength. If the size parameter is greater than ten, then we can assume that the extinction efficiency is close to 2. Therefore, from an experimental knowledge of the extinction coefficient and the volume fraction, the mean diameter of the coal particles can be calculated. This calculated diameter is then compared to the actual mean diameter of the given size

Fig.11 Chart recordings of transmission readings for five different wavelengths. First value corresponds to voltage reading when there are no coal particles, the second value is the averaged (over 2 min) reading when coal is flowing through the test-cell. The ratio of these two values give the spectral transmissivity.

1 1211.18 mV
2 1131.10 mV

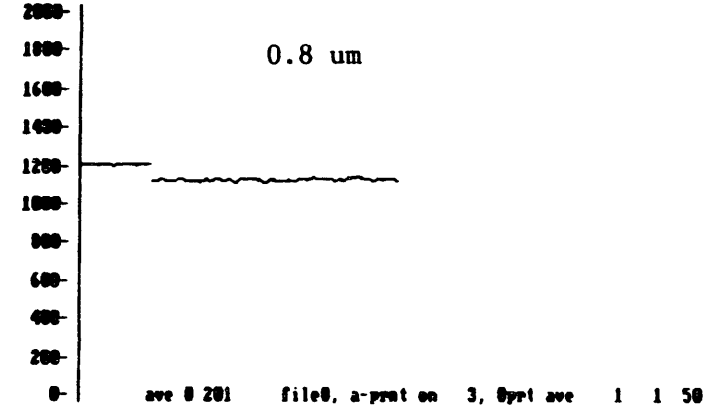

3 1555.70 mV
4 1[illegible] mV

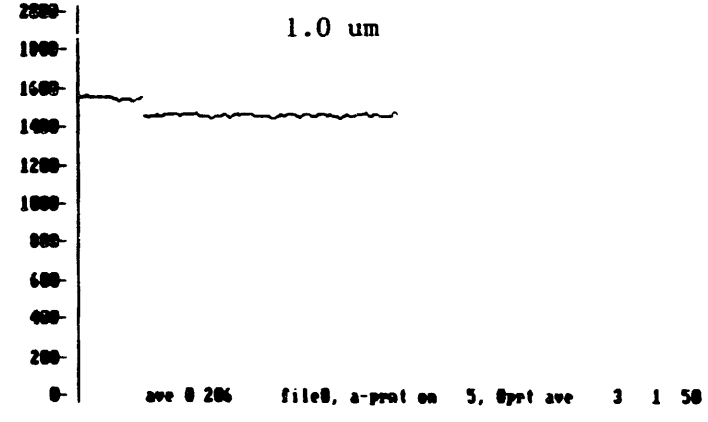

5 1[illegible] mV
6 1[illegible] mV

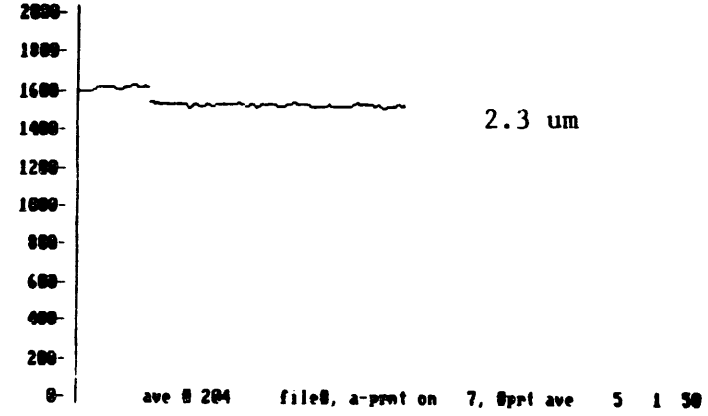

7 1520.12 mV
8 1438.17 mV

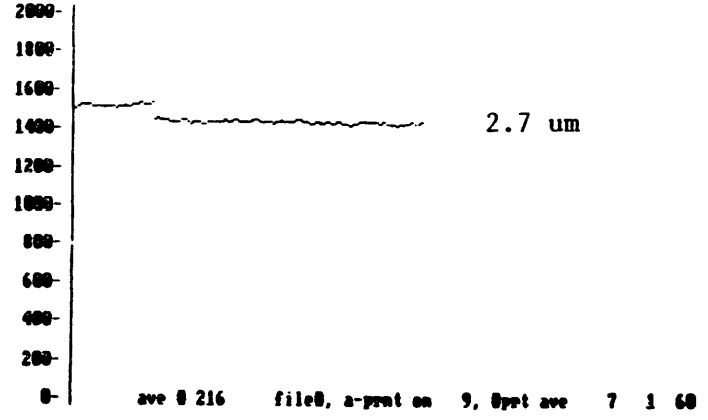

9 794.97 mV
10 747.20 mV

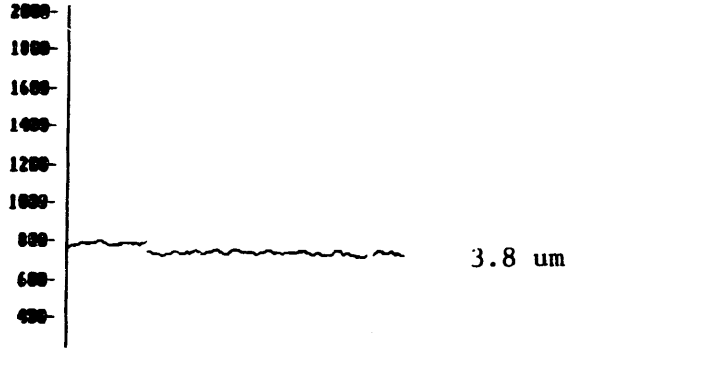

Table 3 Effective diameter predictions based on simple analytical relation. Q_e is assumed to equal to 2. f_v is calculated independently.

Run #1 - 9/23/88

	0.8 microns	1.0 microns	2.3 microns	2.7 microns	3.8 microns
T	0.934	0.942	0.946	0.946	0.940
τ	0.0684	0.0592	0.0558	0.0554	0.0620
β	17.10 /m	14.81 /m	13.96 /m	13.85 /m	15.49 /m
Fv	0.274E-03	0.231E-03	0.214E-03	0.197E-03	0.188E-03
D	48 μm	47 μm	46 μm	43 μm	36 μm

Run #2 - 9/23/88

	0.8 microns	1.0 microns	2.3 microns	2.7 microns	3.8 microns
T	0.934	0.924	0.902	0.889	0.823
τ	0.0684	0.0785	0.1028	0.1172	0.1945
β	17.10 /m	19.63 /m	25.71 /m	29.30 /m	48.64 /m
Fv	0.281E-03	0.277E-03	0.296E-03	0.300E-03	0.286E-03
D	49 μm	42 μm	35 μm	31 μm	18 μm

Run #3 - 9/23/88

	0.8 microns	1.0 microns	2.3 microns	2.7 microns	3.8 microns
T	0.921	0.927	0.905	0.917	0.919
τ	0.0819	0.0754	0.1002	0.0863	0.0846
β	20.47 /m	18.84 /m	25.04 /m	21.58 /m	21.14 /m
Fv	0.274E-03	0.274E-03	0.277E-03	0.274E-03	0.268E-03
D	40 μm	44 μm	33 μm	38 μm	38 μm

distribution to check the accuracy of the experimental results. Once all the errors are corrected, the size distribution of the coal particles will be taken into consideration and the actual extinction efficiency can be determined.

In Table 3, the calculated effective diameters of different particle clouds for three different experimental conditions are shown. In general, the results are consistent. The main source of the error here is the volume fraction of coal particles, because we could not obtain the exact value for the air volume flow rate. Currently, modifications on the experimental cell are made to have more reliable readings for air speed at the exit. On the other hand, it is important to note the spectral trend observed in the results. If we can use the correct values of D_p in calculations, we can get spectral extinction efficiency factor for the coal particles.

4 FUTURE WORK

In the near future, we will complete the preliminary work on the analytical models for the inverse problem. Currently, we have two distinct objectives in this area. One of them is to develop a one-dimensional inverse solution algorithm for homogeneous media. This algorithm will be directly used to reduce the data obtained from no-flame experiments discussed before. Although no details are given in this report, the formulation of this problem is completed, and computer simulations have already been started. The second objective is to implement the formulation of the angular tomography concept and then to evaluate its accuracy experimentally.

We started experiments on this project in May, 1988. In the first round of experiments, we attempted to determine the radiative properties of latex particles and compare our predictions against the available data. Later, we checked the possibility of using the new phase function approximation in data reduction schemes. After that, we started working on one-dimensional pulverized-coal flow experiments. Flame experiments will be started after we obtain extensive data from cold-flow experiments. The third year of the project will be devoted to the development of a data bank for the radiative properties of coal particles. This computerized data bank will list the radiative properties of coal particles as functions of coal rank, size, size distribution,

temperature, and will also give effective size and complex index of refraction that may be used to obtain the required properties from the Lorenz-Mie theory.

5. REFERENCES

Altenkirch, R.A., Peck, R.E., and Chen, A.L., (1979), *Combustion Science and Technology*, Vol.20, pp.49-58.

Atkins, J.T., (1965), "Absorption and scattering of light in turbid media", PhD. Thesis, University of Delaware; (Dissertation abstracts, 1327, no. 6, p. 1844).

Barber, P. and Yeh, C., (1975), "Scattering of electromagnetic waves by arbitrarily shaped dielectric bodies", *Applied Optics*, Vol.14, pp.2864-2872.

Barrett, H.H. and Swindell, W., (1981), *Radiological Imaging*, Academic Press, New York.

Bohren, F. and Huffman, D.R., (1983), *Absorption and Scattering of Light by Small Particles*, John Wiley, New York.

Boothroyd, S.A., Jones, R.A., Nicholson, K.W., and Wood, R., (1987), "Light scattering by fly ash particles and the applicability of Mie theory", *Combustion and Flame*, Vol. 69, pp. 235-241.

Brewster M.Q. and Tien, C.L., (1982), "Radiative transfer in packed fluidized beds : Dependent v/s independent scattering", *ASME Journal of Heat Transfer*, Vol. 104, pp. 573-579.

Brewster, M.Q., and Kunitomo, T., (1983), "The radiative properties of particulates in fluidized-bed coal combustion", *The Proceedings of the ASME-JSME Thermal Engineering Joint Conference*, Hawaii, Vol.4, pp.21-26.

Chakravarty, S., Menguc, M.P., Mackowski, D.W., and Altenkirch, R.A., (1988), "Application of Two Inversion Schemes to Determine the Absorption Coefficient Distribution in Flames", to be presented at the 1988 ASME National Heat Transfer Conference, in Houston, Texas, July 1988.

Chen, F.P. and Goulard, R., (1976), "Retrieval of arbitrary concentration and temperature fields by multiangular scanning techniques", *J. Quant. Spectrosc. Radiat. Transfer*, Vol. 16, pp.819-827.

Chylek, P., Grams, G.W., and Pinnick, R.G., (1976), "Light scattering by irregular randomly oriented particles", *Science*, Vol.193, pp.480-482.

Chylek, P., Srivastava, V., Pinnick, R.G., and Wang., R.T., (1988), " Scattering of electromagnetic waves by composite spherical particles : experiment and effective medium approximations", *Applied Optics*, Vol. 27, No. 12, pp. 2396-2404.

Colby, P.C., Narducci, L.M., Bluemel, V., and Baer, J., (1975), "Light scattering measurements from dense optical systems", *Physiacal Review A*, Vol. 12, No. 4, pp. 1530-1538.

Craig, T.D. and Incropera, F.P., (1984), "Radiation transfer in absorbing-scattering liquids : 1. Radiance and flux measurements", *J. Quant. Spectrosc. Radiat. Transf.*, Vol. 31, No. 2, pp. 127-137.

Cremers, C.J. and Birkebak, R.C., (1966), "Application of the Abel integral equation to spectrographic data", *Applied Optics*, Vol.5, pp.1057-1064.

Deans, S.R., (1983), *The Radon Transform and Some of Its Applications*, John Wiley and Sons, New York.

Dezelic, G. and Kratohvil, J.P., (1961), "Determination of particle size of polystyrene latexes by light scattering", *Journal of Colloid Science*, Vol. 16, pp. 561-580.

Duke Scientific Corporation Bulletin, (1983), California.

Faeth, G.M., Jeng, S.-M., and Gore, J., (1985), "Radiation from fires", *Heat Transfer in Fire and Combustion Systems*, Edited by C.K. Law, Y. Jaluria, W.W. Yuen, and K. Miyasaka, ASME HTD-Vol. 45, pp.137-151.

Granatstein,V.L., Rhinewine, M., Levine, A.M., Feinstein, D.L., Mazurowski, M.J., and Piech, K.R., (1972), "Multiple scattering of laser light from a turbid medium", *Applied Optics*, Vol. 11 No. 5, pp. 1217-1223.

Harding, G., (1982), On the sensitivity and application possibilities of a novel Compton scatter imaging system, *IEEE Transactions on Nuclear Science*, Vol. NS-29, pp. 1260-1265.

Herman, G.T., (1980), *Image Reconstructions from Projections*, Academic Press, New York.

Hommert, P.J., Viskanta, R., and Mellor, A.M., (1977) "Flame temperature measurements by spectral remote sensing", *Combustion and Flame*, Vol.30, p.295.

Hottel, H.C. and Sarofim, A.F., (1967), *Radiative Transfer*, McGraw Hill, New York.

Hottel, H.C., Sarofim, A.F., Evans, L.B., and Vasalos, I.A., (1968), "Radiative transfer in anisotropically scattering media : allowance for Fresnel reflection at the boundaries", *ASME Journal of Heat Transfer*, Vol. 90, Feb. 1968, pp. 56-62.

Hottel, H.C., Sarofim, A.F., Vasalos, I.A., and Dalzell, W.H., (1970), "Multiple scatter : Comparison of theory with experiment", *ASME Journal of Heat Transfer*, Vol. 92, pp.285-291.

Hottel, H.C., Sarofim, A.F., Dalzell, W.H., and Vasalos, I.A., (1971), "Optical properties of coatings : Effect of pigment concentration", *AIAA Journal*, Vol. 9, No. 10, pp. 1895-1898.

Howard, F.H., Novotny, J.L., (1974), "Reflectance of a scattering medium containing polydisperse nonspherical particles", *Fifth International Heat Transfer Conference*, Vol. 1, pp. 26-29.

Hussein, E.M.A., Meneley, D.A., and Banerjee, S., (1986), "On the solution of the inverse problem of radiation scattering imaging", *Nuclear Science and Engineering*, Vol.2, pp.341-349.

Iizuka, K., (1985), *Engineering Optics*, Springer Verlag, Berlin.

Incropera, F.P., Wagner, T.R., and Houf, W.G., (1981), "A comparison of predictions and measurements of the radiation field in a shallow water layer', *Water Resources Research*, Vol. 17, No. 1, pp. 142-148.

Ishimaru, A. and Kuga, Y., (1982), "Attenuation constant of a coherent field in a dense distribution of particles", *Journal of Optical Society of America*, Vol. 72, No. 10, pp. 1317-1320.

Kamiuto, K. and Iwamoto, M., (1987), "Combined conductive and radiative heat transfer through a glass particle layer", *Proceedings of the ASME-JSME Thermal Engineering Joint Conference*, Vol. 4, pp. 77-84.

Kerker, M., (1969), *The Scattering of Light*, Academic Press, New York.

Kratohvil, J.P. and Smart, C., (1965), "Calibration of light scattering instruments III. Absolute angular intensity measurements on Mie scatterers", *Journal of Colloid Science,* Vol. 20, pp. 875-892.

Kurosaki, Y., Take-uchi, M., Kashiwagi, T., and Yamada, J., (1987), "Development of measuring method for radiative properties of fibrous porous media", *Proceedings of the ASME-JSME Thermal Engineering Joint Conference,* Vol. 4, pp. 319-325.

Leadder, J.C. and Dalton, W.A.J., (1975), "Polarisation dependence of EM scattering from Rayleigh scatterers embedded in a dielectric slab. 2.- Experiment", *Journal of Applied Physics,* Vol. 46, No. 10, pp. 4386-4391.

Look, D.C., Nelson, H.F., Crosbie, A.L., and Dougherty, R.L., (1978), "Two-dimensional multiple scattering : Comparison of theory with experiment", *Transactions of the ASME, Vol. 100, Aug. 1978, pp. 480-485.*

Look, D.C., Nelson, H.F., and Crosbie, A.L., (1981), "Anisotropic two-dimensional scattering : Comparison of experiment with theory", *ASME Journal of Heat Transfer,* Vol. 103, pp. 127-134.

Love, T.J., (1968), *Radiative Heat Transfer,* C.E. Merrill Publishing Company, Columbus, OH.

Janzen, J., (1980), "Extinction of light by highly nonspherical strongly absorbing colloidal particles : Spectrophotometric determination of volume distributions for carbon blacks", *Applied Optics,* Vol. 19, No. 17, pp. 2977-2985.

Mackowski, D.W., (1987), "Investigation of the Radiative Properties of Chain Agglomerated Soot formed in Hydrocarbon Diffusion Flames", Ph.D. Thesis, Department of Mechanical Engineering, University of Kentucky, Lexington, Kentucky.

Margolis, J.S., McCleese, D.J., and Hunt, G.E., (1972), "Laboratory simulation of diffuse reflectivity from a cloudy planetary atmosphere", *Applied Optics,* Vol. 11, No. 5, pp. 1212-1216.

Menguc, M.P. and Viskanta, R., (1986), "A sensitivity analysis for radiative heat transfer in a pulverized-coal fired furnace", *Combustion Science and Technology,* Vol.51, Nos 1&2, p.51.

Menguc, M.P., (1988), "Tomographic Reconstruction Technique for Axisymmetric, Anisotropically Scattering Media", Unpublished notes.

Menguc, M.P. and Subramaniam, S., (1988), "Step-Eddington Phase Function Approximation", to be submitted to *Applied Optics.*

Mewes, D. and Ostendorf, W., (1986), "Application of tomographic measurement techniques for process engineering studies", *International Chemical Engineering,* Vol. 26, No.1, pp.11-21.

Nelson, H.F., Look, D.C., and Crosbie, A.L., (1986), "Two dimensional radiative back scattering from optically thick media", *ASME Journal of Heat Transfer,* Vol. 108, pp. 619-625.

Nelson, H.F. and Satish, B.V., (1987), "Transmission of a Laser Beam Through Anisotropic Scattering Media", *J. Thermophysics and Heat Transfer,* Vol. 1, No. 3., pp. 233-239.

Nelson, H.F. and Satish, B.V., (1988), "Radial Scattering of a Laser Beam in Anisotropic Scattering Media", *J. Thermophysics and Heat Transfer,* Vol. 2, No. 2, pp. 104-109.

Ostendorf, W., Mayinger, F., and Mewes, D., (1986), "A tomographical method using holographic

interferometry for the registration of three-dimensional unsteady temperature profiles in laminar and turbulent flow", *Proceedings of the Eighth International Heat Transfer Conference*, San Fransisco, CA, pp.519-524.

Pinnick, R.G., Carroll, D.E., and Hofmann, D.E., (1976), "Polarized light scattered from monodisperse randomly oriented aerosol particles : measurements", *Applied Optics*, Vol. 15, No. 2, pp. 384-393.

Querfield, C.W., Kerker, M., and Kratohvil, J.P., (1972), "Multiple scattering in a synthetic foggy atmosphere - Experimental results", *Journal of Colloid and Interface Science*, Vol. 39, No. 3, pp. 568-582.

Ramachandran, G.N., and Lakshminarayanan, (1971), Three-dimensional reconstruction from radiographs and electron micrographs: application of convolutions instead of Fourier transform, *Proceedings of National Academy of Science, USA*, Vol.68, pp.2236-2240.

Rangayyan, R., Dhawan, A.P., and Gordon, R., (1985), "Algorithms for limited-view computed tomography: An annotated bibliography and a challenge", *Applied Optics*, Vol. 24, pp.4000-4012.

Ravichandran, M. and Gouldin, F.C., (1986), " Determination of temperature and concentration profiles using (a limited number of) absorption measurements",.ul Combustion Science and Technology, Vol.45, pp.47-64.

Santoro, R.J., Semerjian, H.G., Emmerman, P.J., and Goulard, R., (1981), "Optical tomography for flow field diagnostics", *International Journal of Heat and Mass Transfer* , Vol. 27, pp. 1139-1150.

Santoro, R.J., Semerjian, H.G., and Dobbins, R.A., (1983), "Soot particle measurements in diffusion flames", *Combustion and Flame*, Vol.51, pp. 203-218.

Sarofim, A.F., Hottel, H.C., and Fahimian, E.J., (1968), "Scattering of radiation by particle layers", *AIAA Journal*, Vol. 6, No. 12, pp. 2262-2266.

Slezak, S.E. and Buckius, R.O, (1983), "Dust concentration measurement probe using beta attenuation", *Rev. Sci. Instrum*, Vol. 54, pp. 618-625.

Smart, C., Jacobsen, R., Kerker, M., Kratohvil, J.P., and Matijevic, E., (1965), "Experimental study of multiple light scattering", *Journal of the Optical Society of America*, Vol. 55, No. 8, pp. 947.

Snyder, R. and Hesselink, L., (1985), "High speed optical tomography for flow visualization", *Applied Optics*, Vol. 24, pp.4046-4051.

Tien, C.L., Yamada, Y., and Cartigny, J.D., (1986), "Radiative transfer with dependent scattering by particles : Part 2. Experimental investigation", *ASME Journal of Heat Transfer*, Vol. 108, pp. 614-618.

Uchiyama, H., Nakajima, M., and Yuta, S., (1985), "Measurement of flame temperature distribution by IR emission computed tomography", *Applied Optics*, Vol.24, p.411.

Van de Hulst, H.C., (1981), *Light Scattering by Small Particles*, John Wiley and Sons, New York.

Vest, C.M., (1985), Tomography for properties of materials that bend rays: a tutorial, *Applied Optics*, Vol.24, pp.4089-4094.

DATE
FILMED
9/20/93
END